Review aerticle: some transport phenomena in classical liquids and neutron scattering

Karl-Erik Larsson[a]
[a] Royal Institute of Technology, Stockholm, Sweden

PLEASE SCROLL DOWN FOR ARTICLE

Review Article

Some Transport Phenomena in Classical Liquids and Neutron Scattering

KARL-ERIK LARSSON

Royal Institute of Technology, S-10044 Stockholm, Sweden

Our knowledge in liquid physics and particularly in the field of non-equilibrium phenomena has increased enormously during the last two decades. The reasons are two-fold: (a) the application of the slow neutron inelastic scattering technique to the liquid state has supplied us with very valuable fundamental data and has stimulated theoretical work and (b) the application of molecular dynamics computations to problems of liquid dynamics has profoundly deepened our understanding of fundamental dynamical quantities. The combination of the two ways of research has shown how to approach the solution of classical questions: For instance to what small wave length domain may we apply the normal hydrodynamical equations? And when these equations cease to exist what would be a good theoretical continuation into the short wave length domain? The modern techniques have shown that normal hydrodynamics is useful down to wave lengths approximately ten atomic distances. Thereafter kinetic effects of atomic nature take over. It is also shown that periodic waves are transmitted through insulator liquids like argon and neon to wave lengths of the abovementioned order whereas periodic waves with wave lengths of order two atomic distances are transmitted through liquid metals like rubidium and lead. The questions are associated with the possible *collective motions* in a fluid.

A similar question has to do with *self motion*: It is known that Einsteins relation $\overline{x^2} = 2Dt$ describing the time evolution of the diffusive motion of a particle in a fluid is an asymptotic relation valid for times long compared to for instance atomic or molecular collision times. But to what shorter length of time is the relation valid? Neutron scattering studies combined with molecular dynamics computations and kinetic theory indicates that the range of validity of the Einstein relation extends down to times of order $(6–8) \cdot 10^{-13}$ s corresponding to root-mean-square displacements of order 0.5 Å. This conclusion seems to be valid within an accuracy of approximately 20%.

INTRODUCTION

In the year of 1982 fifty years have passed since the detection of the neutron. This particle has contributed to science and technology in the most spectacular way. Specially the field of slow neutron scattering has contributed profoundly to our knowledge of atomic ordering and dynamics. Lattice dynamics obtained a revival by use of the neutron scattering technique round 1955–60.

Our knowledge of the quantum liquids HeII and He^3 depends to a large and important degree on neutron scattering results collected from 1957 to present day.

Before the application of this fruitful technique to the field of classical liquids the theory of liquid dynamics was rudimentary. During the last 25 years the neutron scattering results on simple classical liquids has been the firm ground upon which new models and theories were built. Due to the fact that the application of computer science in molecular dynamics happens to be useful to simulate atomic motions in liquids within the same space and time region within which neutrons give information, the coupling neutron scattering — molecular dynamics has been most fruitful. In this review a simplified and short account is given of the broad field of liquid dynamics as seen from the horizon of a neutron experimentalist who has taken part in the whole development of neutron scattering since 1955.

1   Fluctuations and neutrons

The atoms and molecules in matter are never at rest. This has been observed for at least 100 years and formed the basis for the kinetic theory of gases constructed by Boltzmann. It was possible in the past to derive a number of transport constants and other macroscopic properties of solids, liquids and gases on the basis of the firm belief that atoms are moving. Such derived properties were diffusion coefficients, viscosity coefficients, specific heats etc. Some other constants were associated with equilibrium properties of the body under observation it may be a solid, liquid or gas.

The existence of deviations from equilibrium — fluctuations — was also known early. In some cases these fluctuations give spectacular results in the form of coherent motions like phonons in solids or elementary excitations in quantum liquids. Theoretically the understanding of lattice vibrations is good and also there is a well developed theory for dilute gases. In between are the states of dense fluids — classical liquids and dense gases — which until recently were not well understood microscopically. Macroscopically the hydrodynamic equations were used to describe the long wave length and low frequency dynamics of fluids. But there was no bridge over to the microscopic dynamics on the atomic level.

In general it was always difficult to observe the fluctuations. Scattering experiments offered a possibility. For instance light scattering allows a study of the Rayleigh and Brillouin scattering intensity in liquids.

With the event of neutron scattering the situation was completely changed. This was first noted by van Hove 1954.[1] The reason that the neutron differs from a light quantum or an X-ray quantum is its mass. According to the de Broglie relation a neutron of wave length of order atomic spacing in

TABLE I

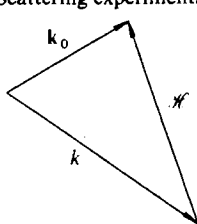| Particle	Energy (E) wave length (λ) relation	Typical wave length and energy	
Neutron	$\lambda = \dfrac{h}{\sqrt{2mE}}$	$\lambda = 1.8\ \text{Å}$	$E \sim 0.025\ \text{eV}$
X-ray	$E = \dfrac{hc}{\lambda}$	$\lambda \sim 1\ \text{Å}$	$E \sim 10^4\ \text{eV}$
Light quantum	$E = \dfrac{hc}{\lambda}$	$\lambda \sim 6000\ \text{Å}$	$E \sim 1\ \text{eV}$

In dense matter:
Atomic separation $\sim 1\ \text{Å}$
Vibrational energies $\sim 0.025\ \text{eV}$

condensed matter has an energy corresponding to typical thermal vibration energies, $k_B T$. This is not the case with X-rays or light quanta according to the scheme in Table I.

Therefore in a scattering experiment a fairly complete mapping in energy, $\hbar\omega$, and in momentum, $\hbar\kappa$, can be performed with neutrons. With X-rays only the spectra in momentum space are easily observable and with light only energy spectra for very small momentum transfers as indicated in the approximate scheme in Table II.

With the present neutron spectroscopic instruments and their normal resolutions this makes the neutron capable of observing fluctuations within

TABLE II

Scattering experiments:

k_0, k = ingoing and scattered wave vectors resp.

$k = \dfrac{2\pi}{\lambda}, k_0 = \dfrac{2\pi}{\lambda_0}$

$k - k_0 = \kappa$ = scattering vector

θ = scattering angle

$E_{\text{out}} - E_{\text{in}} = \pm\hbar\omega$

Observation possibilities:

Particle	Important wave vector (κ) and energy ($\hbar\omega$) range	
Neutron	$\kappa \sim 1\ \text{Å}^{-1}$	$\hbar\omega \sim 0.025\ \text{eV}$
X-ray	$\kappa \sim 1\ \text{Å}$	
Light quantum	$\kappa \sim 10^{-3}\ \text{Å}^{-1}$	$\hbar\omega \sim 10^{-5}\ \text{eV}$

a time range 10^{-11} to 10^{-14} s and a space range from 10 to 0.1 Å. These are exactly the interesting ranges of time and space during which important fluctuations in many cases relax within condensed systems, or during which the single binary collisions or many body collisions occur in a gas of different density. In certain extreme experimental arrangements such as back scattering arrangements and in small angle scattering apparatus other ranges in space and time are possible to reach but are of smaller interest in our present context.

Van Hove also showed that from the statistical mechanics point of view it is a correlation function $G(\mathbf{r}, t)$ which tells about the life of fluctuation. Classically $G(\mathbf{r}, t)$ describes the probability of finding an atom at $\mathbf{r}$ and t if there was an (other or same) atom at the origin at $t = 0$. In the neutron scattering process it is not space and time we learn about. Rather the neutron carries information about momentum and energy transferred to it by the fluctuations.

What is directly measured in the scattering experiment is the doubly differential cross section

$$\frac{\mathrm{d}^2\sigma}{\mathrm{d}\Omega\mathrm{d}\omega} = a_x^2 \frac{k}{k_0} S(\kappa, \omega), \tag{1}$$

where the nuclear properties of the scatterer enter only into the value of the scattering length a_x, which is equal to a_{coh} for coherent scattering and a_{inc} for incoherent scattering. k and k_0 are the values of the outgoing and ingoing wave vectors respectively, and the factor k/k_0 is a measure of the ratio of scattered to ingoing flux in scattering. All the physical properties of the atomic many body problem involved in the scattering process are hidden in the scattering function $S(\kappa, \omega)$, in which $\hbar\kappa$ and $\hbar\omega$ are the momentum and energy changes in the scattering process respectively. As shown by van Hove the relation between $S(\kappa, \omega)$ and $G(\mathbf{r}, t)$ is

$$S(\kappa, \omega) = \frac{1}{(2\pi)^2} \iint e^{i(\kappa\mathbf{r} - \omega t)} G(\mathbf{r}, t)\, \mathrm{d}\mathbf{r}\, \mathrm{d}t \tag{2}$$

This is for the case of coherent scatterer for which collective motions are revealed in the scattering process. When the nuclear properties are such that only incoherent scattering occurs a similar formula holds with $S(\kappa, \omega)$ replaced by $S_s(\kappa, \omega)$ and $G(\mathbf{r}, t)$ replaced by $G_s(\mathbf{r}, t)$ the index s denoting that in this case only self motion of a single scattering atom is observed.

As indicated in Figure 1 van Hove gave a very clear picture of the physical interpretation of $G(\mathbf{r}, t)$ and $G_s(\mathbf{r}, t)$. In general $G(\mathbf{r}, t)$ is described as a sum

$$G(\mathbf{r}, t) = G_s(\mathbf{r}, t) + G_d(\mathbf{r}, t), \tag{3}$$

where $G_d(\mathbf{r}, t)$ describes the dynamical correlation between pairs of particles in the many-body medium and $G_d(\mathbf{r}, 0)$ is the well known static pair correlation function $g(\mathbf{r})$. As time goes on all of the functions smears out such that
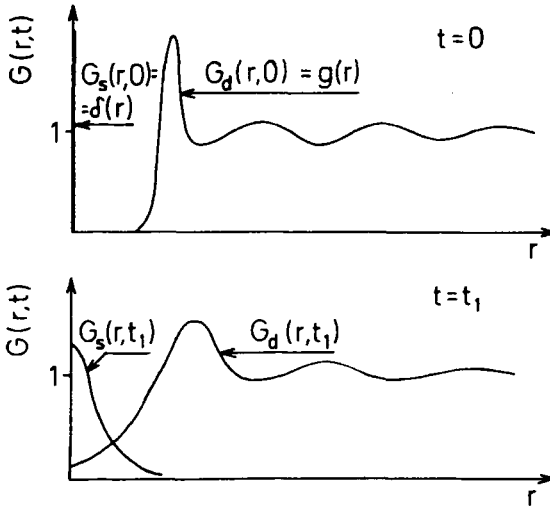
FIGURE 1   Van Hoves picture of the time evolution of the self and pair correlation functions $G_s(r, t)$ and $G_d(r, t)$, respectively. Here exemplified at $t = 0$ and at a later time $t = t_1$.

$G(\mathbf{r}, t)$ tends to 1 for very large times. This means that the fluctuation is completely relaxed.

Particularly for the self motion asymptotic forms for time intervals long and short compared to the elementary interaction times between atoms or molecules in the medium, let us say a fluid, were formulated by Vineyard[2] namely the simple diffusion approximation valid as $t \rightarrow \infty$

$$G_s(\mathbf{r}, t) = \frac{1}{(2\pi \overline{x^2(t)})^{3/2}} e^{r^2/2\overline{x^2(t)}}, \tag{4}$$

where the Gaussian approximation for the spreading out of a particle in space is invoked and $\overline{x^2(t)}$ is the mean square deviation discussed by Einstein

$$\overline{x^2(t)} = 2Dt. \tag{5}$$

This gives for $S_s(\kappa, \omega)$ the frequently used formula

$$S_s(\kappa, \omega) = \frac{1}{\pi} \frac{D\kappa^2}{(D\kappa^2)^2 + \omega^2} \tag{6}$$

valid only for *long* times corresponding to small ω. For very *short* times, $t \rightarrow 0$, the force action between particles may be neglected and a description of free motion always valid in a very dilute gas is approached, namely

$$\overline{x^2} = \tfrac{1}{2}(v_0 t)^2 \tag{7}$$

leading to

$$S_s(\kappa, \omega) = \frac{1}{2\pi\kappa v_0} e^{-1/2(\omega/\kappa v_0)^2}, \tag{8}$$

where $v_0^2 = k_B T/m$, symbols having their usual meanings. These two limit-
ing forms have found a frequent use in the analysis of neutron scattering
experiments.

Returning to the introductory remarks regarding the wide range of energy
and momentum changes in the scattering process covered by the neutron,
it so happens that the main part of the dispersion relations for phonons in
solids fall within the neutron window (Figure 2a). Similarly the neutron in
principle makes it possible to find out if collective modes similar to the
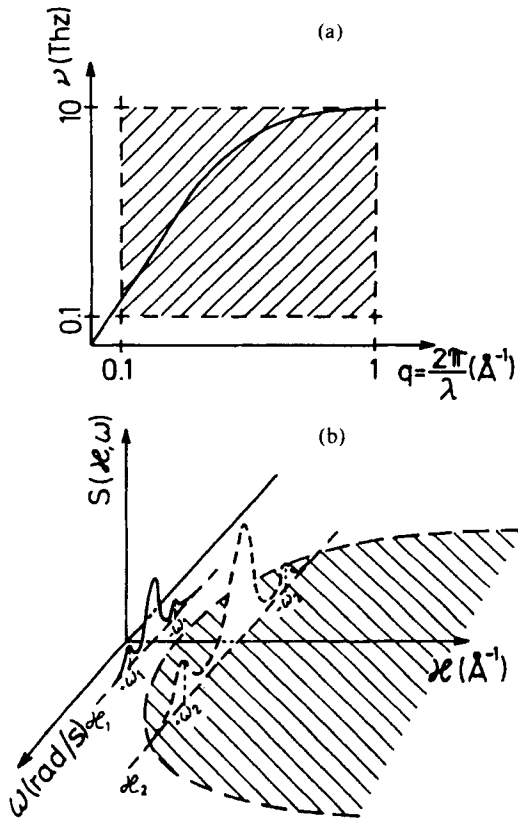

FIGURE 2 Approximate extension of neutron window (shaded area) in κ and ω within
which scattered neutrons are able to carry information about dynamical processes: a) in a
periodic solid structure, where phonons can be observed within the most important wave
vector—energy region and b) in a liquid or dense gas, where it was already earlier known that
at very long wave lengths (~ 1000 Å) and low frequencies ($\sim 10^{-2}$ Thz) a light scattering
picture shows the two typical features the quasielastic Rayleigh peak and the inelastic Brillouin
peak in which the scattered quantum is shifted by $\omega_1 = \pm c\kappa_1$, where c is the sound velocity.
The neutron may show to what higher frequency domain ($v_2 \sim 1$ Thz, $\lambda_2 \sim 6$ Å) this principal
picture can be pushed. Available area approximately given by $10 > \kappa_2 > 0.01$ Å^{-1}, $0 <
|\omega_2| < 10^{14}$ rad/s.

hydrodynamic modes of motion in a liquid or gas persists for smaller wave lengths and higher frequences (Figure 2b). Furthermore the possibilities to study the effects of collisions at different densities in the system under investigation are very good (Figure 3). If we now concentrate on fluid systems it is obvious that neutron scattering offers a chance to investigate the range of validity of hydrodynamics down in space and time towards atomic magnitudes. For distances smaller than or for the order of atomic distances, and times of order time between collisions, we expect kinetic effects to take over. Neutrons have offered an ideal tool to investigate such effects. The main difficulty is to understand and interpret in detail the rich information carried by the scattered neutron.

In the following chapters a review is presented of the evolution of our understanding of fluid dynamics as it has evolved during the era of neutron
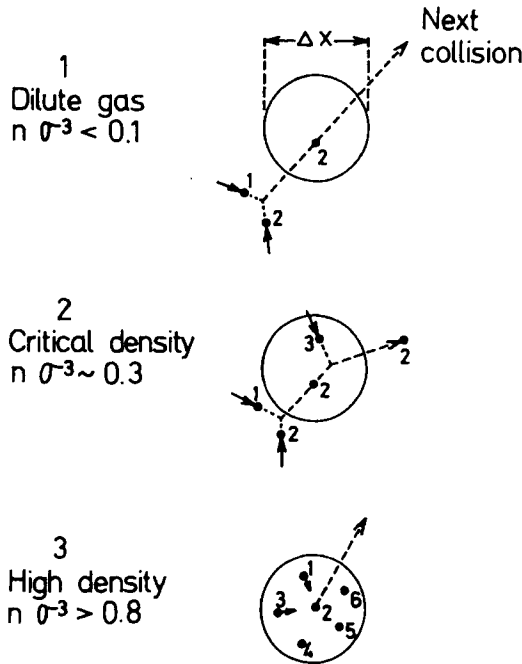

FIGURE 3 Applying the uncertainty relation, $\Delta p \Delta x \geq \hbar$, to the magnitudes involved in a neutron scattering process, one finds if $\Delta p = \hbar \kappa$ that $\Delta x \geq 1/\kappa$. One may say that the neutron acts like a microscope with an aperture $1/\kappa$. Within this aperture the neutron observes different phenomena depending upon (a) density of the system given by $n\sigma^3$, where $n =$ number density and σ is an effective atomic diameter, which together determine the mean free path (l) between collisions and (b) upon the aperture, Δx, given by $1/\kappa$. The critical parameter is $\Delta x/l \sim 1/\kappa l$. 1, 2, etc. are molecules. In a dilute gas (case 1) the neutron observes free flight, in a medium dense gas (case 2) the neutron may observe a binary collision and parts of free flights and in a dense gas (case 3) it observes a collective collision.

inelastic scattering from about 1957–58 to 1982, a period of 25 years. It is shown how the neutron measurements together with the new use of computers during the period in the form of molecular dynamics opened particularly the field of liquids to firmer theory construction. Before 1958 very little was known on the atomic theory of liquids dynamics. A very great number of research workers contributed to the development of ideas, theories and experiments during these 25 years. In what follows only a few of all these papers will be cited namely those which according to the opinion of the author in some respect were fundamental to our understanding or which were of pioneering importance.

2 Early observations and models for liquid dynamics

Van Hoves theoretical work was known but maybe not fully appreciated before 1960. If we now concentrate on fluid systems what have we learnt during the two decades that passed since then? Let us first begin with the period up to about 1968–1970. The thinking during the years, 1959 to 1968, was dominated rather much by an early observation. In 1958 studies of phonon processes in an aluminium single crystal at elevated temperatures were performed by Larsson et al.[3] Similar studies were performed by Brockhouse on a lead crystal.[4] From these studies a broadening of the single phonon resonance lines was observed (Figure 4). Multiphonon contributions were also studied and compared to phonon expansion formulas. Interpreting this broadening as an effect of damping the mean life of the phonon could be calculated from the uncertainty relation. It was found (Figure 5) that the mean life time and the mean free paths determined from the width observation was of order 1.5 times the phonon wave length near the melting point.

The next step was to take a polycrystalline sample.[5] In that case one would expect scattering to occur only between certain limits determined in principle by the numbers $\tau + q$ and $\tau - q$, where τ is a reciprocal lattice vector and q is a phonon wave vector. A gap between ingoing neutron energy and the scattered intensity may be created by the existence of (1) a reciprocal lattice and (2) a phonon spectrum with a dispersion relation (Figure 6). The experimental result on the polycrystalline sample taken near the melting point confirms the prediction, valid under the experimental circumstances selected, i.e. no Bragg peak falling under the ingoing spectrum range (Figure 7a).

The interesting question is now what happens if we let the sample melt. The experiment was performed and the result was startling.[5] (Figure 7b). The difference between the liquid spectrum and the polycrystalline one is minimal. It was known that the spectrum from the poly-crystal was created by damped phonons plus a multiphonon contribution and it suggests itself to ask whether
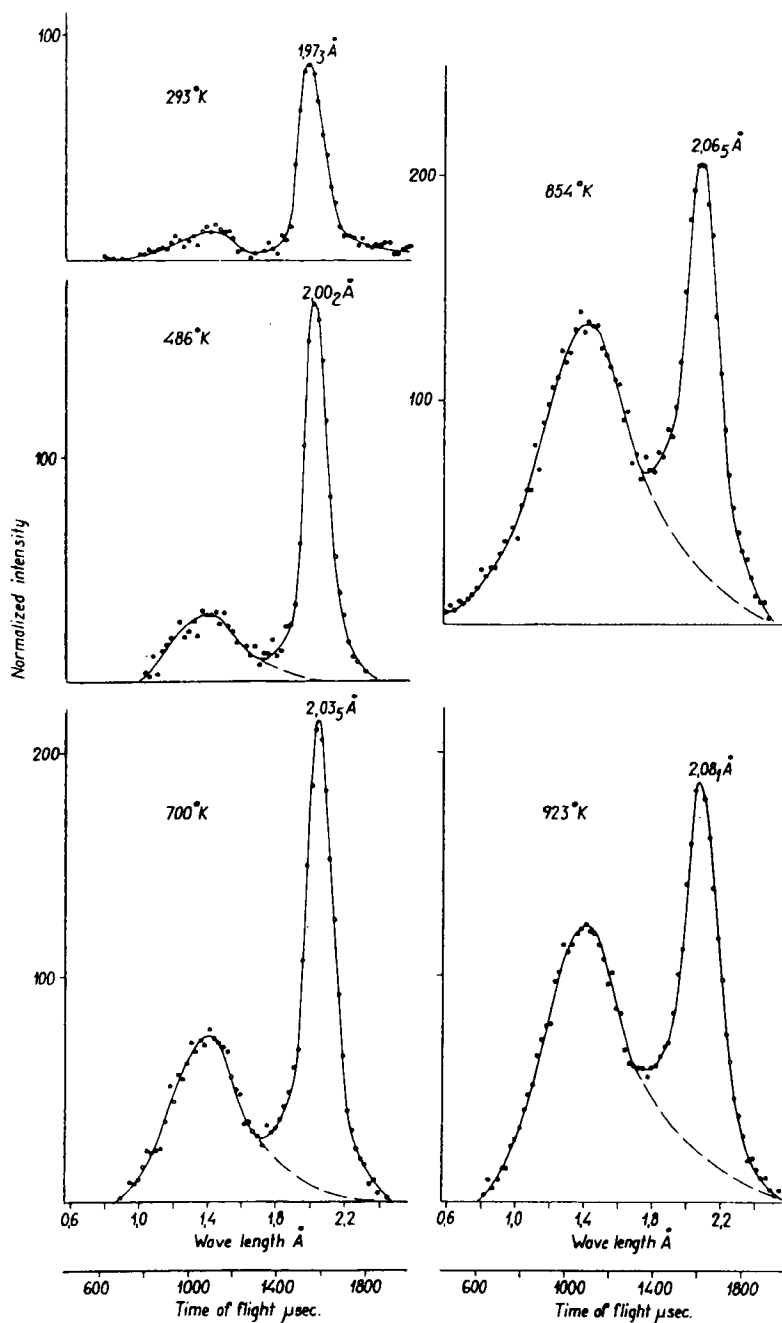
(a)

FIGURE 4   a) Single phonon resonance line plus the multi-phonon spectrum observed for a particular orientation of a single aluminium crystal at temperatures from 293 to 923°K. Melting point is at 933°K. The ingoing neutron wave length is ~ 4 Å ~ 5 meV or at a time-of-flight of 3000 μs. The wave length and frequency of the observed phonon group is ~ 6 Å and ~ 5 Thz.
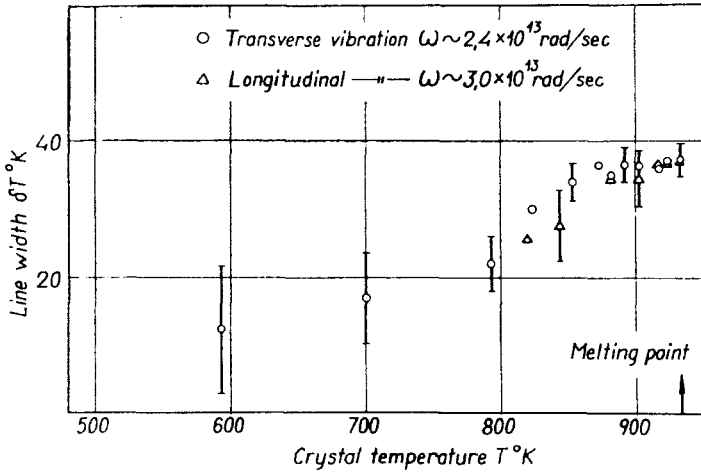
281

FIGURE 4   b) Observed phonon line broadening as a function of temperature for two different phonon groups (after K. E. Larsson, U. Dahlborg and S. Holmryd, 1960).

such damped excitations exist also in the liquid phase. The question was raised: Do collective excitations exist in a liquid at the high frequencies and the short wave lengths we are now considering, i.e. $10^{12} - 10^{13}$ Hz and 3–10 Å resp.?

No theories existed that could be of value in this situation. From the hydro-dynamic equations Brillouin peaks were expected at much smaller frequencies and wave lengths in the macroscopic domain involving "volume elements" instead of single atoms. Already in 1958 Vineyard[2] had proposed his con-volution approximation to describe the scattering function $S(\kappa, \omega)$. To construct $S(\kappa, \omega)$ Vineyard used the formula $G(\mathbf{r}, t) = G_s(\mathbf{r}, t) + G_d(\mathbf{r}, t)$ and for $G_d(\mathbf{r}, t)$ he used the ansatz

$$G_d(\mathbf{r}, t) = \int g(\mathbf{r}')G_s(\mathbf{r}, - \mathbf{r}')\, d\mathbf{r}', \qquad (9)$$

which leads to the scattering function

$$S(\kappa, \omega) = S(\kappa)S_s(\kappa, \omega), \qquad (10)$$

where $S(\kappa)$ is the liquid static structure factor. What the basic ansatz amounts to is to assume that the correlation hole round any atom moves rigidly with the atom. There is no collective motion possible. Also the existence of the central atom given by $G_s(\mathbf{r}, t)$ is not taken into account. Such a model could not possibly be used to understand the data.

It was speculated that the main fault with Vineyards idea was that occurring at small r's. *The motion of the distinct atom is not influenced by the presence*
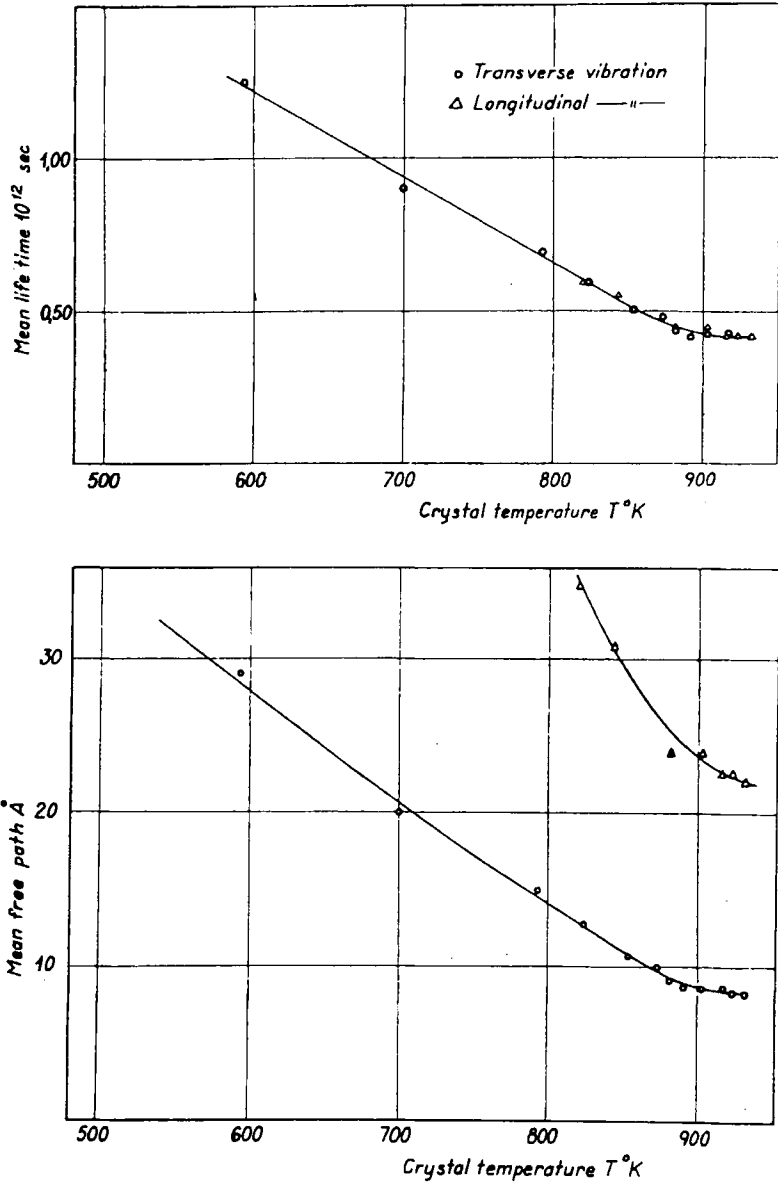
FIGURE 5   Phonon mean life time and mean free paths derived from the observed widths of the phonon groups (after K. E. Larsson, U. Dahlborg and S. Holmryd, 1960).
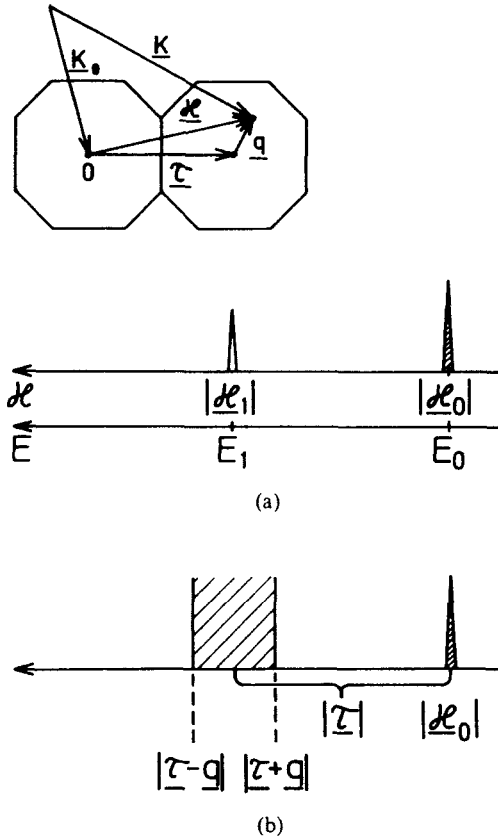
FIGURE 6   a) Scattering vector diagram for single crystal. τ is reciprocal lattice vector and q phonon wave vector. The simultaneous relations to be fulfilled are $\mathbf{k} - \mathbf{k}_0 = \mathbf{q} + \tau$; $(\hbar^2/2m)(k^2 - k_0^2) = \pm k\omega$ and $\omega = \omega(\mathbf{q})$. The scattering pattern is assumed to contain one phonon line at κ_1 or energy E_1. Ingoing wave vector values is κ_0 and neutron energy E_0. b) To obtain the allowed intensity region scattered from a poly crystal we rotate the figure a) round the point 0 and let q be oriented parallel and anti-parallel to τ. We then obtain allowed intensity to be observed in a range $\tau + q > \kappa > \tau - q$ (shaded region).

of the atom at the origin at $t = 0$. Singwi[6] formulated the mathematics of the idea that one should assume the almost extreme opposite: assume that within our fluctuating liquid the atoms surrounding the atom at the origin perform a motion highly correlated with the central one (Figure 8). Their motion was described as phonon motion within a sphere of coherence of radius R. Outside this sphere the atoms may be assumed to move as described in the convolution approximation for instance in a diffusive manner with due regard taken to the structure of the liquid. There is thus a correction to the

(a)
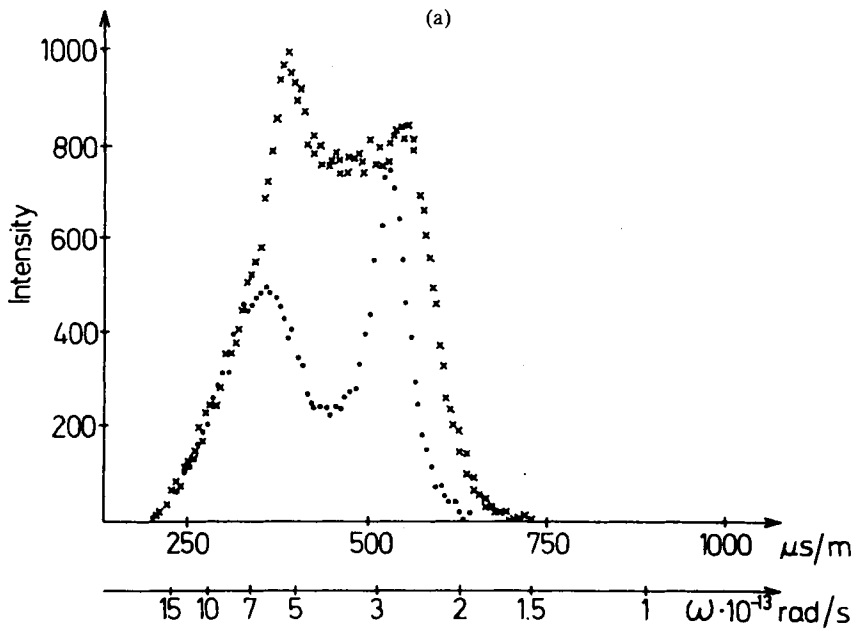
FIGURE 7 a) Neutron intensity scattered from a single crystal (.....) and from poly-crystalline sample (xxxx) of aluminium at 903°K. Melting point at 933°K. Ingoing neutron spectrum at 1000 μs/m and longer flight times. Intensity gap from 1000 μs/m to about 650 μs/m caused by the lattice periodicity.
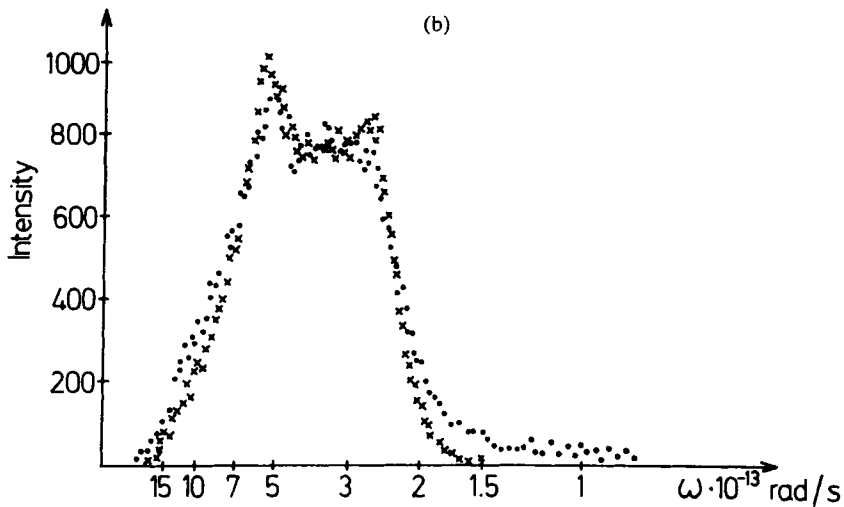

(b)

FIGURE 7 b) Neutron intensity scattered from a poly-crystalline sample (xxxx) at 903°K and from a liquid sample at 950°K (....). Both observations performed at constant angle of observation, 60°, and with berylliumfiltered neutrons ingoing (after K. E. Larsson, U. Dahlborg and D. Jovic (1965)).
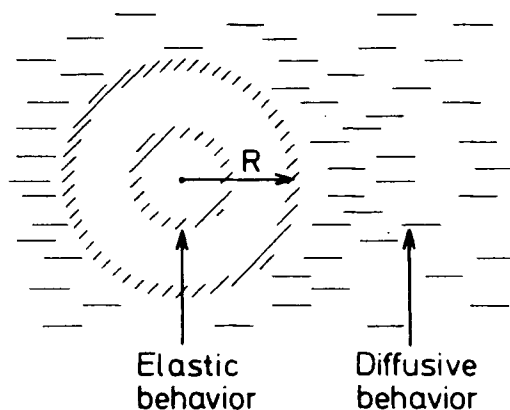
FIGURE 8 The basic physics of atomic motion in simple liquids as guessed by Singwi in the early 1960's on basis of neutron scattering results. R is a range of coherence of motion round each atom including a few neighbour rings within which elastic behaviour dominates.

Vineyard approximation such that the scattering function is now

$$S(\kappa, \omega) = S(\kappa)S_s(\kappa, \omega) + H(\kappa, \omega) = S_s(\kappa, \omega)\left[S(\kappa) + \frac{1}{6}\left(\frac{\omega}{c}\right)^2 L(R, \kappa, q)\right]$$

(11)

Here H or L are correction factors and q is the quasi-phonon wave number belonging to frequency ω. c is sound velocity.

Even more drastically solid-like models for liquid atomic motion were invented by Egelstaff.[7] We notice in passing that the Singwi ansatz has much in common with the physical ideas behind the so called mean field approximation or with visco-elastic theories developed later. According to the mean field theory the atoms round a certain atom moves in concert — but notice: without any special care being taken to the central atom and its possible strong interaction with neighbours for instance in a binary collision.

Such models as Singwis and Egelstaffs were tested against new and more extensive measurements on two widely different liquids namely liquid lead[9] and liquid argon.[8] When we now turn to the comparison between experiments and models we notice that these new experiments were performed at higher flux reactors. The used neutron fluxes increased from $3 \cdot 10^{12}$ to 10^{14} n/cm^2 s as exemplified by the Stockholm reactor, $R1$, on the one hand with flux 10^{12} and the Idaho Falls materials testing reactor (MTR) or the Studsvik reactor $R2$ in Sweden in the flux range of 10^{14} n/cm^2.s. on the other hand. The first liquid aluminium studies were made with a flux of 10^{12} and cold neutrons whereas the subsequent studies on liquid lead and liquid argon were made with the 10^{14} flux level and in addition to cold neutrons, thermal neutrons were also used. As a result of the higher available

flux a more complete mapping of $S(\kappa, \omega)$ could be made such that $S(\kappa, \omega)$ could be studied for constant κ or constant ω over the entire range of values of these variables as the situation was in the 1960:ies. This means that $S(\kappa, \omega)$ could be studied over that range of κ for which the liquid structure factor $S(\kappa) = \int S(\kappa, \omega) \, d\omega$ has a value close to one. Thus very small κ-values, for which $S(\kappa) \ll 1$, were excluded from study.

If one inspects data from these days, ~ 1965, one may do many interesting observations. If we have a look at corrected lead data by Randolph and Singwi[9] we see first of all that no inelastic peaks are observed in these plots of the differential cross section at constant angle of observation (Figure 9). No collective modes show up as peaks within the κ-region investigated. If there exist such modes they must be thoroughly smeared out like in a poly-crystal. One reasoned that in order to compare to models like the Singwi model valid for single phonon processes one would have to subtract from the observed pattern the effect of multiphonon scattering. And now for the first time one also could begin to correct in an approximative way for multiple scattering in the sample container. Such corrections were attempted already in the end of the 1950's by Brockhouse and Pope.[10] The importance
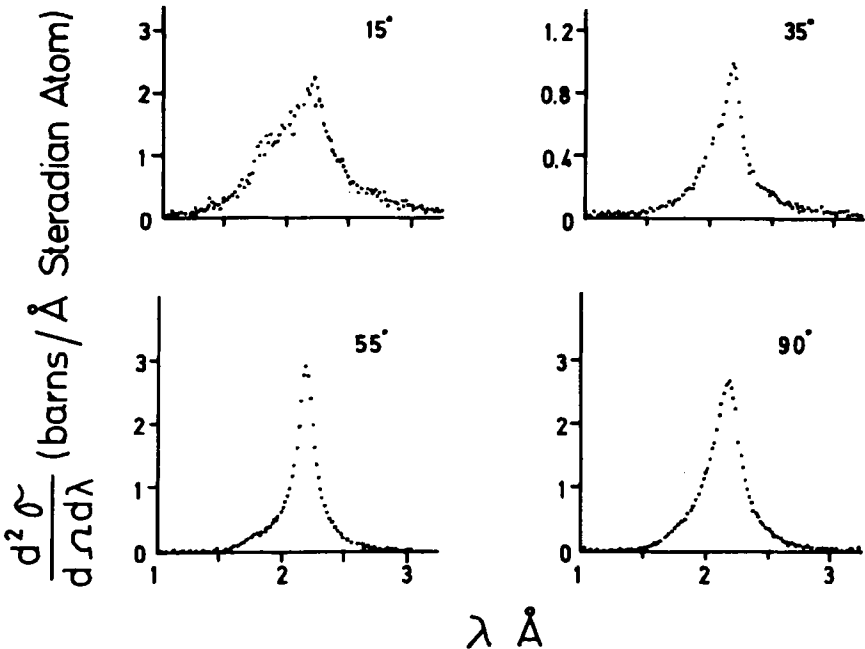

FIGURE 9   Partial differential cross section for neutron scattering from liquid lead at 625°K as a function of scatterred-neutron wave length at various constant angles of observation (after P. D. Randolph and K. S. Singwi (1966)).

of this correction did not become clear until much later in the 1970's. First when these two corrections were performed could a comparison to theoretical models be made. One observed that the convolution approximation is bad and that the Singwi model fits a little better. The critical parameter is the Singwi correction factor. This can be calculated and it can be directly extracted from the experiment by comparison with the convolution model. Having established what R-value is most reasonable one finds that to each constant ω only one value of q fits the data and one in such a way obtained a dispersion relation $\omega = \omega(q)$.
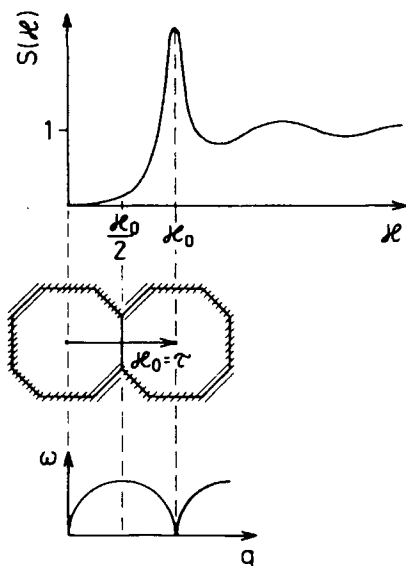
FIGURE 10   The main peak at κ_0 of the liquid structure factor $S(\kappa)$ was considered as a generalized Bragg peak. This allows a construction of a corresponding generalized Brillouin zone picture with a second zone centered at κ_0 which plays the role of a reciprocal lattice vector τ. In such a picture it is logic to refer the derived $\omega(q)$ values (pairs of ω and q belonging together) to this second generalized Brillouin zone.

   But now we come to a critical point. From what point should the dispersion relation be drawn? In a solid with its regular atomic arrangement in a periodic lattice we may construct Brillouin zones such that when a phonon gets a wave number or wave vector larger than $\tau/2$ it is referred to the next zone, in the center of which we have a Bragg peak. So the phonons are referred to the closest Bragg reflection (compare Figure 6). In the spirit of this model and remembering the similarity between Singwis approach and the dynamics in a solid (solid-like model) one considers the first peak of the liquid structure factor as a generalized Bragg peak (Figure 10). Therefore

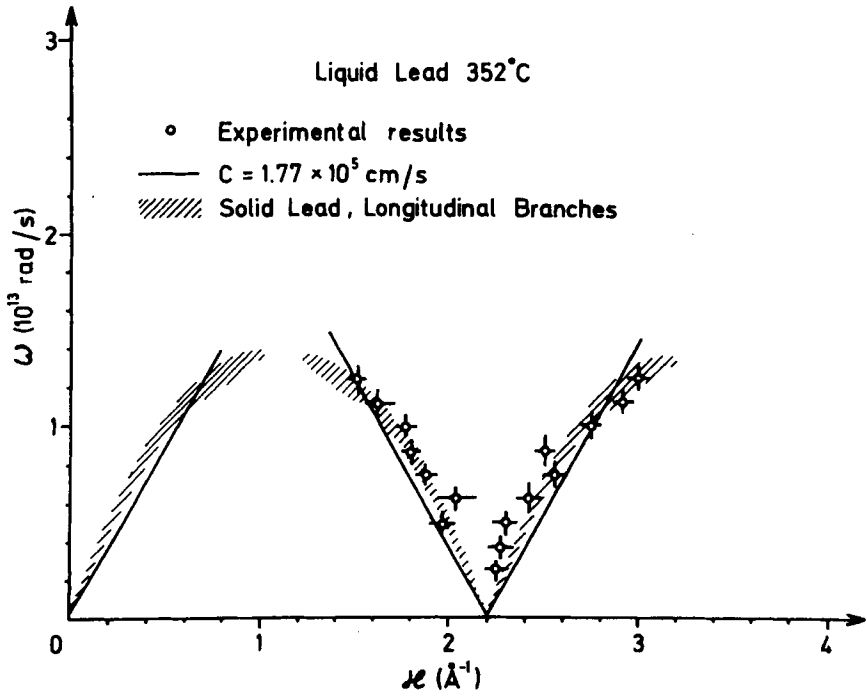FIGURE 11 The dispersion curve for liquid lead derived by Randolph and Singwi from the data of Figure 9. Observe that $\kappa = 2.2\,\text{Å}^{-1}$ is considered as a Bragg point in a reciprocal lattice (after Randolph and Singwi, 1966).

the derived (ω, q) were plotted round the κ-value of this peak, $2.2\,\text{Å}^{-1}$ (Figure 11). This result represents the ultimate in this era of believing in a solid-like behaviour of liquid dynamics. Observe that a periodic dispersion relation is assumed even without having seen an inelastic peak. On the other hand we have the knowledge that the high temperature polycrystalline and liquid energy spectra looked very similar. The dispersion curve must therefore have related to an average phonon in the liquid. $g(\mathbf{r})$ has only *one* strong peak corresponding to a sphere of nearest neighbours and the following spheres are rather badly defined. The lack of clear periodicity reflects in the relatively undefined and broad main peak in the structure factor $S(\kappa)$ as compared to the sharp Bragg plots from the solid. It is therefore to be expected that the highest frequency excitations, if they exist, are strongly damped, perhaps within a distance of order two atomic distances. The important feature in the dynamical events may even be the very first collision, the binary event. In such a case it is hard to speak about single excitations as periodic motions. Such questions remained to be answered.

3   Indications of a new era

Round 1960 or soon thereafter computers started their impact on the field of liquid theory and on treatment and interpretation of neutron scattering data. Until the middle of 1960's and even much longer—it is fair to say even today—the neutron scattering studies are plagued by the phenomenon of multiple scattering. Even if the sample container is constructed with the aim to reduce such effects, for instance by use of strongly absorbing spacers, the multiple scattering is the main hindrance from extending neutron scattering studies to such regions in (κ, ω)-space which are of importance for finding single excitations, i.e. the small κ-region. This is also a region of great interest for structure factor determinations and the attempts to derive an effective pair potential from this structure factor. Other regions which remain undetermined are the large ω-regions where also $S(\kappa, \omega)$ takes on small values. This has so far for instance prevented experimental determinations of the fourth frequency moment of the scattering function which contains information on the force between atoms. However, during the 1970's the art of computing multiple scattering from known cross sections and compositions and shapes of sample container and sample have become feasible. A breakthrough in this respect was created by Copley and first applied to scattering studies of liquid rubidium[11] (1974). Earlier good correction work was performed for liquid argon[17] and later very careful multiple scattering calculations were made in several studies (liquid lead,[27] bismuth[38]). The method of subtracting the multiple scattering component requires a reliable absolute determination of the cross section. The earlier *factor method* suffers from the weakness of being model dependent.[12] A new philosophy in shaping the sample containers also contributes in reducing multiple scattering.

The computers also, have revolutionized the field in another way. During the 1970's it has become possible to compute even the most involved mathematical expressions describing theoretical values of the scattering functions. Examples are offered by modern mode-coupling theories. Similarly by the aid of the computer accurate comparisons between theory and experiment have become feasible even if very extended data collections are obtained.

Still another important contribution from computer, from the theoretical point of view, is the possibility to perform molecular dynamics studies. By solving Newtons equations of motion for a very large number of particles, say 1000, in a box moving under the action of a known potential it is possible to describe positions as function of time and thereby to find the van Hove correlation functions or their Fourier transforms under the given premises. Of equal or even greater importance is that other magnitudes such as velocity correlation functions and their memory functions, current correlation func-

tions etc. may be found from such studies. On the whole, features which are not directly observable by neutron scattering may be studied in detail.[13-15]

To understand why molecular dynamics has become so valuable it is useful to consider a few basic theoretical developments describing deep-going statistical mechanics quantities.[12,16] It was mentioned above that the self motion, $G_s(\mathbf{r}, t)$ if often approximated by a Gaussian function of width $\overline{x^2}(t)$. It may be shown that

$$\overline{x^2(t)} = 2 \int_0^t dt'(t - t') \langle v_x(0)v_x(t') \rangle, \tag{12}$$

where $\langle v_x(0)v_x(t) \rangle$ is the velocity auto correlation function. The scattering function measured in a neutron scattering experiment $S_s(\kappa, \omega)$ is obviously a very complex function of the velocity correlation function hidden in the width $\overline{x^2}(t)$. In order to obtain $\overline{x^2}(t)$ from such a measurement one would have to take the Fourier inverse to obtain $F_s(\kappa, t)$. It has been shown that the Gaussian assumption in itself is not quite correct just in the time domain round $5 \cdot 10^{-13}$ to $5 \cdot 10^{-12}$s, where neutrons are most effective to observe atomic motions. A non-Gaussian correction should — at least sometimes — be made. It is thus still more difficult to obtain information on $\langle v_x(0)v_x(t) \rangle$ from a neutron scattering experiment. Furthermore it is only from an observation of $S_s(\kappa, \omega)$ that one could derive $\overline{x^2}(t)$. Incoherently scattering liquids do practically not exist (vanadium the only exception). Mixtures of coherent and incoherent exist and several metals are pure coherent scatterers. By use of isotope separated samples it is possible to obtain $S_s(\kappa, \omega)$ if-say-one isotope scatters mainly coherently and an isotope mixture may be realized such that incoherent scattering dominates. Such an example is A–36 (coherent) and A–40 + A–36 (mainly incoherent).[17] Argon is the only insulator substance for which $S_s(\kappa, \omega)$ was experimentally determined in an objection free way simulataneously as $S(\kappa, \omega)$ was determined. Similarly a study[18] of liquid nickel was performed using a mixture of nickel–58 and nickel–62. In this way parts of the separated scattering surfaces for a liquid metal were found.

There is a great deal of interest in $\langle v_x(0)v_x(t) \rangle$ because deeper developments in statistical non equilibrium mechanics deal with it.
The Langevin diffusion equation is well known

$$M \frac{d\mathbf{v}(t)}{dt} = -\xi \mathbf{v}(t) + \mathbf{R}(t) \tag{13}$$

It is, however, to be considered as an equation of motion for a large sphere moving in a fluid of smaller particles, like the simple diffusion equation analogue (Einsteins idea). The internal friction coefficient and the diffusion coefficient, D, are connected via the relation, $\xi = k_B T/MD$. When we decrease the dimension of the sphere down to atomic sizes and consider the

corresponding short times, we have to generalize the equation. The friction constant is transformed into a time dependent transport coefficient ($\xi/M = \gamma \rightarrow \gamma(t)$), which has been named a memory function (discussed already by Landau). A simple memory function equation results for $\langle v(0)v(t)\rangle$:

$$\frac{d}{dt}\langle \mathbf{v}(0)\mathbf{v}(t)\rangle = -\int_0^t \gamma(t - t')\langle \mathbf{v}(t')\mathbf{v}(0)\rangle\, dt' \qquad (14)$$

It leads to the well known results of Langevin diffusion for a δ-function form of the memory and to an oscillating behaviour for a constant memory (Figure 12a). By this description we have in fact brought into consideration the possible visco-elastic behaviour of a liquid (Figure 12b). This seems quite promising as a working hypothesis remembering the slight solid-like behaviour of some liquids. The first thoughts in this direction were presented by Maxwell and may be described as follows:[19] when a disturbance in a fluid is slow compared to its natural relaxation time it responds to the disturbance with viscous flow and if it is very rapid it responds more or less like a solid with elastic vibrations. The memory function is thus a magnitude of greatest interest. It can in principle be derived from molecular dynamics data by numerical solution of the integro-differential equation for $\langle v_x(0)v_x(t)\rangle$.

(a)

(b)

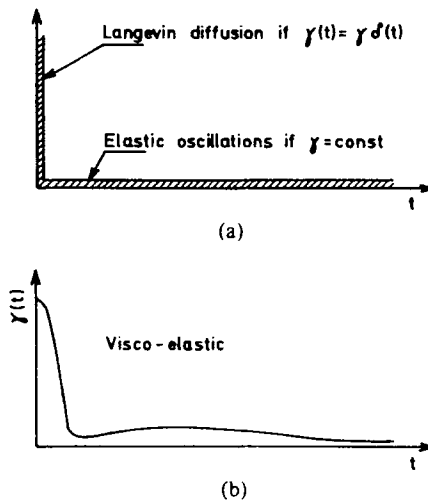FIGURE 12   a) Principal shapes of memory function leading to the two extreme cases of motion namely (1) the random Langevin diffusion process if $\gamma(t) = \gamma\delta(t)$ (= no memory at all) and (2) elastic vibrations if $\gamma(t) = \gamma$ (= a memory that remains constant forever). b) Memory function for a realistic case of a liquid showing visco-elastic atomic dynamics, which contains ingredients of both the extreme cases.
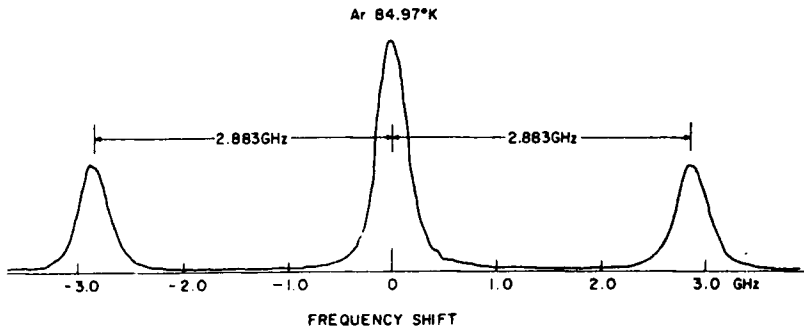
FIGURE 13 Experimentally obtained light scattering picture by scattering laser light of wave length 5145 Å from liquid argon at 85°K. A central Rayleigh peak and the two displaced Brilloin peaks are clearly seen (after P. A. Fleury and J. P. Boon, 1969).

A further theoretical development along these lines has taken place from 1963 (Kadanoff & Martin).[20] Zwanzig[21] and co-workers have systematically developed the scheme of *generalized hydrodynamics*. The reason for these efforts is simple: Any theory describing liquid dynamics should in the limit of long wave lengths (small κ) and low frequencies (small ω) transform into the predictions of the hydrodynamic equations, which describe conservation of mass, momentum and energy in fluid motion. For a long wave length radiation like light these equations predict that in a scattering process three intensity peaks should be observed: the central Rayleigh and the shifted Brillouin peaks. Such spectra have been observed (Figure 13). The widths of the peaks, i.e. the damping of the fluctuations, are determined by $\chi = K/\rho_0 C_p =$ the thermal diffusivity for the central peak and by $\Gamma = \frac{1}{2}[v_l + (\gamma - 1)\chi]$ for the side peaks. $v_l =$ longitudinal kinematic viscosity and $K =$ coefficient of thermal conductivity. $\rho_0 v_l = \frac{4}{3}\eta_s + \eta_B$, where $\eta_s =$ shear and $\eta_B =$ bulk viscosity. $\gamma = C_p/C_v =$ specific heat ratio. One should remember that the fluid is considered as a continuous medium; it is locally homogenous and isotropic, viscous and thermally conducting. The transport coefficients are considered as *constant* parameters.

The normal hydrodynamic description will break down when the fluctuations considered have wave lengths of order atomic distances and corresponding high frequencies. We expect that the viscous behaviour should be replaced by a visco-elastic one. The transformation of the macroscopic hydrodynamics to a microscopic generalized hydrodynamics is performed by use of the sum rules. A useful way of illustrating how the transform is performed is to consider the longitudinal current correlation function.

Our main aim is to investigate what happens to the collective motions in the fluid known as sound waves when the wave length is gradually decreased down to atomic dimensions. In for instance light scattering these show up

as the Brillouin doublet peaks occurring for $\omega = \pm c_{ad}\kappa$, where c_{ad} = the adiabatic sound velocity. If such peaks exist also for wave lengths of atomic dimensions they should be of a nature related to the phonons in solids, which were observed to exist up to the melting point of the solid in a strongly damped form. If temperature fluctuations are neglected the longitudinal part of the linearized Navier–Stokes equation is

$$\frac{\partial}{\partial t} j_l \mathbf{r}, t = -\frac{1}{M}[\nabla p(\mathbf{r}, t)_l + v_l \nabla^2 j_l(\mathbf{r}, t)] \tag{15}$$

where $j_l(\mathbf{r}, t)$ is the longitudinal current and $p(\mathbf{r}, t)$ the pressure. Instead of considering the current itself it is of interest for the present purposes to con-consider the current correlation or rather its spatial Fourier transform $J_l(\kappa, t) = \langle j^l_{-\kappa}(t) j^l_\kappa(t) \rangle$. This current correlation satisfies the equation[16]

$$\frac{\partial}{\partial t} J_l(\kappa, t) = -\frac{\kappa^2}{nM\chi_T} \int_0^t dt' J_l(\kappa, t') - v_l \kappa^2 J_l(\kappa, t), \tag{16}$$

where χ_T = the isothermal compressibility. The solution of this equation results in a double peaked structure corresponding to the Brillouin peaks but with the sound velocity given by the isothermal one due to the neglect of thermal fluctuations. It may be shown that the application of the zeroth frequency moment of $J_l(\kappa, \omega)$, which is simply = $v_0^2 = k_B T/M$, requires that the isothermal compressibility χ_T be replaced by $S(\kappa)/nk_B T$. The static structure factor $S(\kappa)$ is thus introduced. n is the number density. This means that the constant compressibility factor is replaced by a wave length dependent one, *a non-local compressibility factor*. It may, however, be shown that the second frequency moment of $J_l(\kappa, \omega)$, which is given below as $\omega_l^2(\kappa)$, is not fulfilled even with this shift of meaning of the compressibility factor. In a phenomenological fashion it is therefore guessed that the constant viscosity term v_l must be replaced by a space and time dependent one. Or in our formulation: $v_l \rightarrow \phi(\kappa, t)$. *Such a transformation of the viscosity to a viscosity function is in the spirit of visco-elastic theory.*[21] With these transformations the Navier-Stokes equation for the current correlation is changed to

$$\frac{\partial}{\partial t} J_l(\kappa, t) = -\frac{(\kappa v_0)^2}{S(\kappa)} \int_0^t dt' J_l(\kappa, t') - \kappa^2 \int_0^t dt' \phi_l(\kappa, t - t') J_l(\kappa, t') \tag{17}$$

The application of the second frequency moment of $J_l(\kappa, \omega)$—a static quantity—determines not the full viscosity function $\phi_l(\kappa, t)$ but rather its initial value $\phi_l(\kappa, 0)$, which comes out as

$$\phi_l(\kappa, 0) = \frac{\omega_l^2(\kappa)}{(v_0\kappa)^2} - \frac{v_0^2}{S(\kappa)} \tag{18}$$

It is observed that the force between pairs of atoms is thus introduced via $\omega_l^2(\kappa)$, which is given by

$$\omega_l^2(\kappa) = 3\kappa^2 v_0^2 + \frac{n v_0^2}{M} \int d^3r \, g(r)(1 - \cos \kappa z)\frac{\partial^2 u(r)}{\partial z^2}. \qquad (19)$$

Here $g(r)$ is the static pair correlation function and $u(r)$ is the potential between a pair of atoms.

It should, however, be stressed that *the physics of the relaxation process on the atomic scale is now hidden in the time dependence of $\phi(\kappa, t)$.* The importance of these various steps is that the normal mathematical form of the linearized Navier–Stokes equation is now formally applicable down to the atomic space and time scale. We have not learnt anything new about the relaxation processes themselves and as a matter of fact it remains to be demonstrated that the basic physics of the atomic dynamics is correctly described by this framework. The predictions from this model should for instance be in harmony with the findings from kinetic theory. We return to this question later. Before leaving the transformation to generalized hydrodynamics it should be noticed that the equation arrived at can be written

$$\frac{\partial}{\partial t}J_l(\kappa, t) = -\int_0^t dt' \, K_l(\kappa, t - t')J_l(\kappa, t') \qquad (20)$$

with the memory function $K_l(\kappa, t)$ given by

$$K_l(\kappa, t) = \frac{(\kappa v_0)^2}{S(\kappa)} + \kappa^2 \, \phi_l(\kappa, t). \qquad (21)$$

One has arrived at a form familiar from the Mori theory and applied to the velocity auto correlation function above.

A typical example of application of this theory and combination with molecular dynamics studies is the work by Ailawadi, Rahman and Zwanzig[23] (1971). $J(\kappa, t)$ is computed by molecular dynamics for a Lennard–Jones liquid (argonlike). It is Fourier transformed to give $J(\kappa, \omega)$, which is used for comparison with the calculated $J(\kappa, \omega)$. A Gaussian form was assumed for $\phi(\kappa, t)$ namely $\exp[-\pi t^2/4\tau^2(\kappa)]$. Part of the physics is now hidden in $\tau(\kappa)$ and part in the choice of a Gaussian form. τ was determined by fitting to the molecular dynamics data (Figure 14). The result is that a reasonable fit is obtained between the molecular dynamics results and the prediction from generalized hydrodynamics. It is, however, to be noticed that this fit is obtained at the cost of producing a κ-dependent relaxation time τ. The physical meaning of $\tau(\kappa)$ remains unexplained. A considerably more detailed study was performed by Levesque et al.[14] These authors showed that the modest fit produced by a simple Gaussian memory function could be
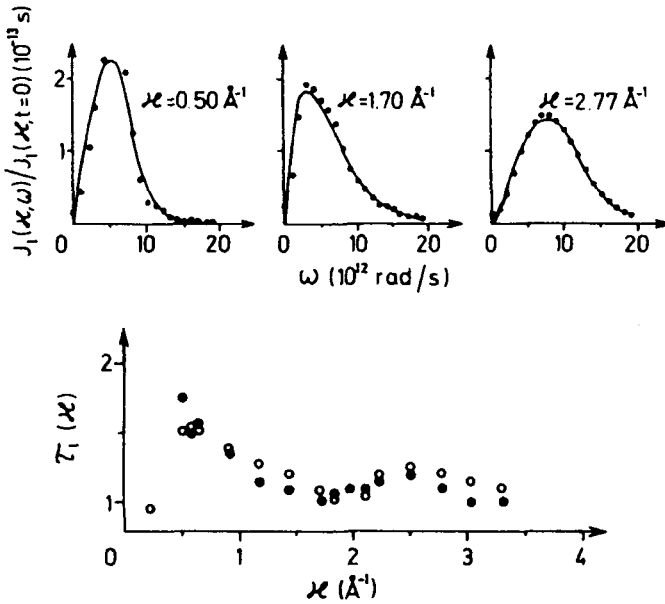
FIGURE 14   In the top part of this figure is shown the longitudinal current correlation
function obtained from molecular dynamics calculations (filled circles). The full lines represent
the same quantity as calculated from generalized hydrodynamics with a Gaussian form of the
memory function and with the width parameter $\tau(\kappa)$. The derived shape of $\tau(\kappa)$ is shown as the
bottom part of the figure (from N. K. Ailawadi, A. Rahman and R. Zwanzig, 1971).

improved to a more nearly perfect fit-considering the statistical errors in the
molecular dynamics calculations — by introducing a much more complex
memory function. The important conclusion reached by these authors is
that a double relaxation time is necessary to produce a perfect fit, namely a
fast relaxing component plus a slower decaying one.

In this way theory took the molecular dynamics study as the "truth" with
which to compare theory for testing. It is quite common that molecular
dynamics and theory tend to form a couple from which the "truth" is ex-
tracted. It is, however, imperative that the molecular dynamics results are
tested now and then against pure experimental results. In the particular
case of a Lennard–Jones fluid the molecular dynamics have been tested
against modern and accurate liquid argon data, have shown agreement and
should be safe. Using such theories or other similar ones involving the idea
of a visco-elastic nature of short time liquid dynamics, it was possible in the
period around 1970 to generate $S(\kappa, \omega)$ scattering surfaces useful as visual
guides[24] (Figure 15).

It is, however, to be noticed that (1) the physics of $\tau(\kappa)$ or other combina-
tions of parameters remains unexplained. Also (2) it was not proved that the
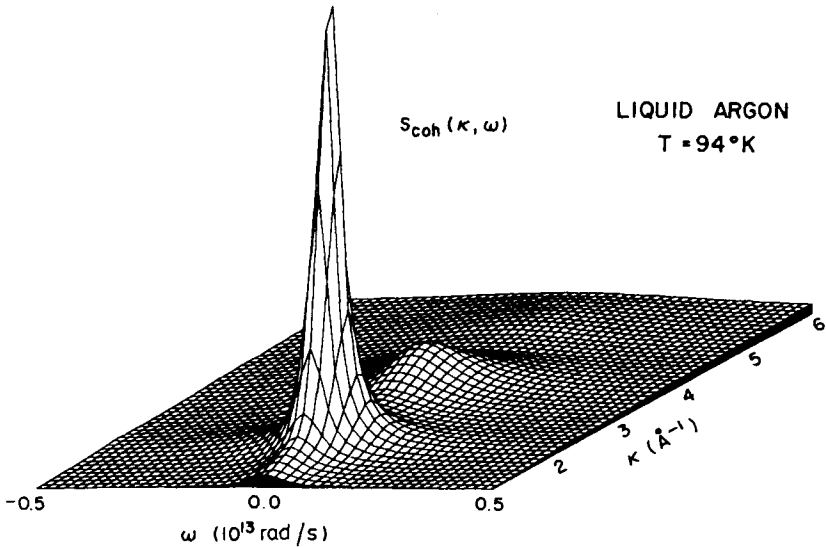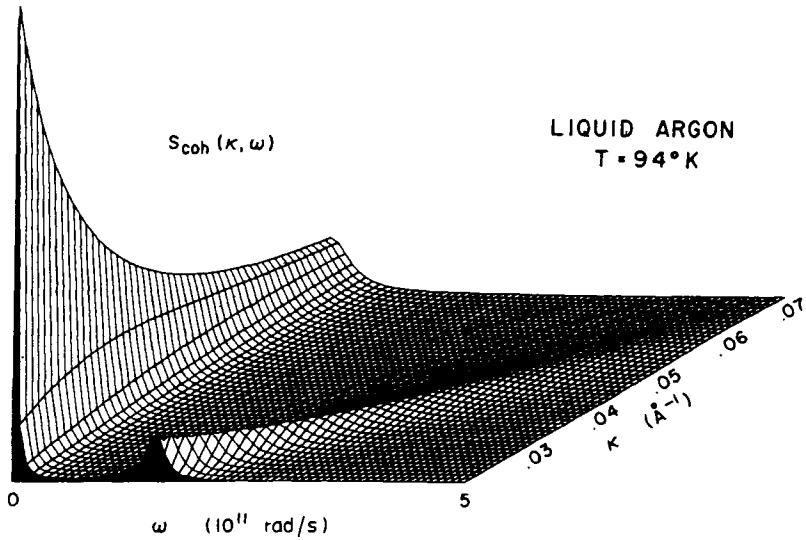
FIGURE 15 The coherent scattering function calculated on the basis of visco-elastic theory for liquid argon at 94°K. The model is characteristic in that it is arranged such that it gives the correct hydrodynamic limit as well as the free particle limit when $\kappa \to \infty$. The first three even frequency moments are used to fix the parameters of the model. The top part illustrates the predicted short range of existence of Brilloin peaks in the small κ domain, whereas the bottom part shows a structure-dominated scattering function in the large κ domain (after Sears, 1970).

physical concepts behind the hydrodynamic framework of formulas is valid at these short wave-lengths. Furthermore (3) it is known that a considerable part of the atomic motion seen in the short wave length region ($\kappa > \kappa_0$) comes from the self motion and there is no such notion as self motion in hydrodynamics.

4   Important experimental results

During the years 1972 to 1982 several accurate and relatively complete experimental mappings of scattering functions were made. The first was a careful scattering study on liquid argon. There was a first study performed in Studsvik, Sweden, by Sköld and Larsson,[8] published 1967, followed by the most complete one performed at the MTR in Idaho Falls 1971 by Sköld et al.[17] (published 1972). It is quite instructive to compare these two studies in which the first one (1967) interpreted data according to various phenomenological models invoking solid-like behaviour of the liquid. In the studies published five years later the generalized hydrodynamics and other visco-elastic theories had replaced the earlier models. In the latter study A–36 was used separately such that $S(\kappa, \omega)$ and $S_s(\kappa, \omega)$ could be separated. The characteristic features of this study is the use of such ingoing neutron energies, (15 and 20 meV), that a rather wide κ-range from 1 to 4.4 Å^{-1} and relatively complete ω-range is observed. The main reason that the study was not carried to smaller κ-values was the difficulty with low intensity and high relative multiple scattering contribution. The magnitude of the calculated multiple scattering shows the importance of performing it correctly (Figure 16). An integration of the intensity in ω-direction gives $S(\kappa)$. A comparison with the separately studied[25] $S(\kappa)$ shows how the difficulties pile up at small κ-values (Figure 17). The final mapping of $S(\kappa, \omega)$ as well as $S_s(\kappa, \omega)$ shows that there are no peaks due to collective excitations in this Lennard–Jones system within the investigated κ-ω-domain (Figure 18). Various models such as the generalized hydrodynamics model were compared to these data with modest success. On the other hand the agreement between the molecular dynamics data of Rahman and Verlet and the experiment is good. We defer the detailed comparison to theory until we have discussed more recent theories. Let us just remember the absence of single excitations at least down to 1 Å^{-1}. Molecular dynamics studies of Leveque et al.[14] indicate that such features are expected only up to about $\kappa \sim 0.3$ Å^{-1}.

A study of interest in order to find experimental evidence for single excitations in liquids is the German work performed at Jülich on fluid neon by Bell et al.[26] published 1975. These experiments were performed on high pressure neon gas at various temperatures between 75° and 45°K and pressures between 120 and a few atmospheres. The density varied between
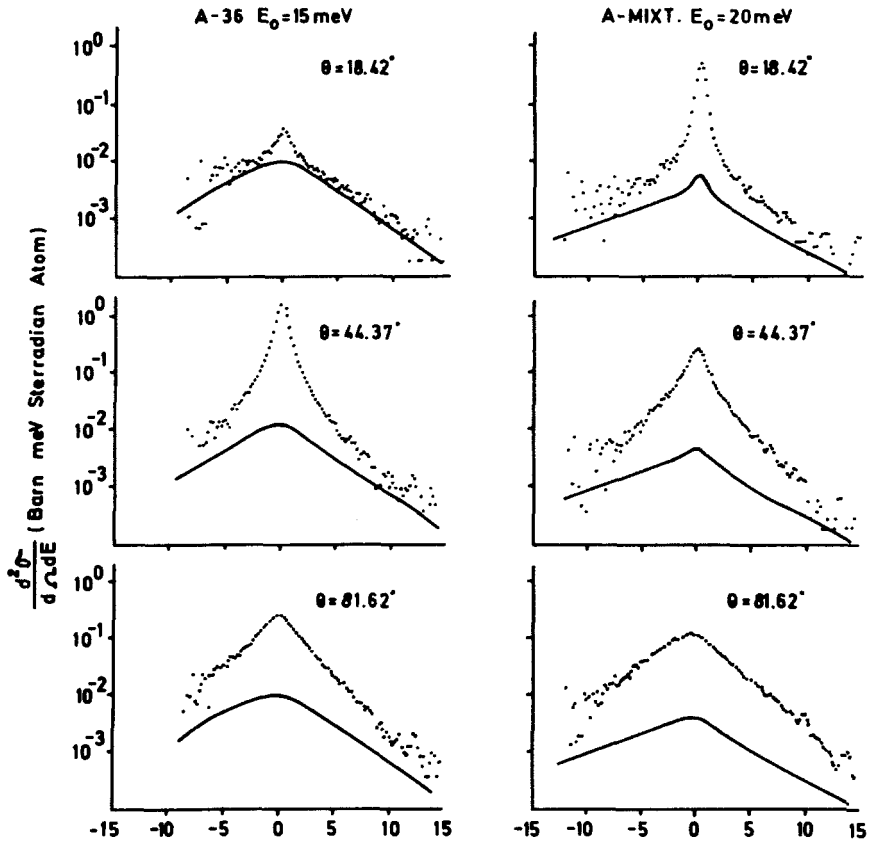
FIGURE 16   Double differential scattering cross section from neutron scattering on liquid argon at 85°K at three constant angles of observation, two different ingoing neutron energies and for the coherent scatterer A-36 and a mixture of A-36 plus A-40 showing both coherent and incoherent contributions. The dots give the experimental results and the solid curves the calculated multiple scattering contributions. The latter ones ones are seen to be very important for large energy transfers (κ-values) (after K. Skold, J. M. Rowe, G. Ostrowski and P. D. Randolph, 1972).

0.98 and 0.34 g/cm^3. The scattering experiments were performed at a triple axis spectrometer in the constant κ mode of operation. By performing the observation at very small angles of observations, 3–7 degrees, and for ingoing energy round 2 MeV these researchworkers were able to observe $S(\kappa, \omega)$ for $0.06 < \kappa < 0.18$ Å^{-1}. Due to the very small ingoing energy even doubly scattered neutrons cannot reach $\kappa = 2.1$ Å^{-1}, which is the value of κ at which the peak of the structure factor occurs. Therefore data are not corrected for multiple scattering. At these small momentum transfers a clearly visible three-peak structure is observed (Figure 19). Above $\kappa \sim 0.15$ Å^{-1} this
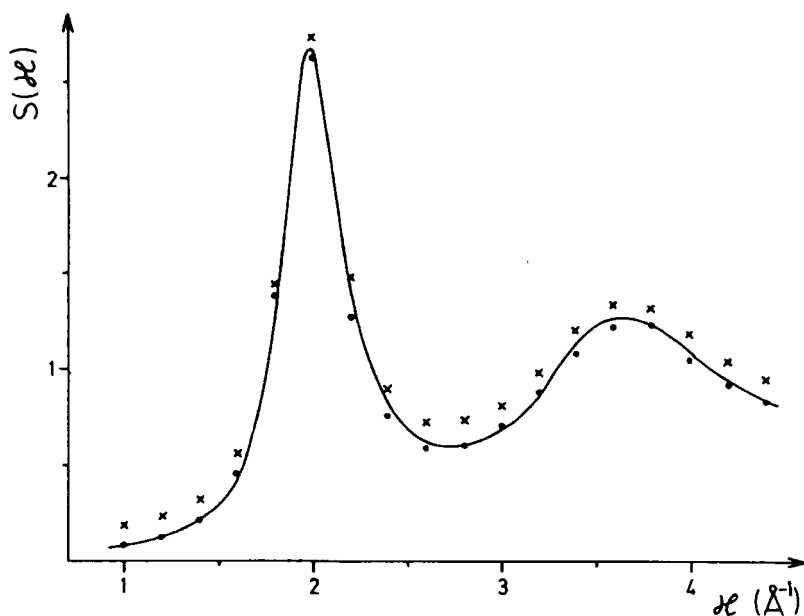
FIGURE 17   The scattering function $S(\kappa, \omega)$ for liquid argon at 85°K integrated over ω for constant κ giving $S(\kappa)$ compared to a separately measured structure factor $S(\kappa)$ (————). (xxxx) = integrated result before multiple scattering correction, (. . . .) = same result after multiple scattering correction. Observe the large correction at small κ-values (after K. Sköld, J. M. Rowe, G. Ostrowski and P. D. Randolph, 1972).

structure disappears. This seems to be in agreement with what is expected for liquid argon. The observed data could be described with the normal hydrodynamic formulas involving constant transport coefficients. This means that the hydrodynamic behaviour in this case ceases at wave lengths of order $2\pi/\kappa$ Å $= 40$ Å. In the case of the argon studies it was derived that $\overline{x^2}(t)$ shows a rather clear diffusion behaviour. This means that if there are any collective modes in argon they should appear in a κ-region where hydrodynamics is valid. In the shorter wave length domain the "grainy" atomic structure dominates. Apparently the structure given by the Lennard–Jones potential does not permit existence of collective high frequency modes.

Except argon and neon there are two liquid metals for which carefully corrected sets of data are presented and which are of interest because they show a behaviour different from Lennard–Jones liquids. These are liquid rubidium[11] and liquid lead.[27]

To start with rubidium[11] this study was made at CP–5 in Argonne by Copley and Rowe in time-of-flight experiments using the ingoing neutron energies 4.94 and 33.9 meV. The cylindrical sample container of aluminium
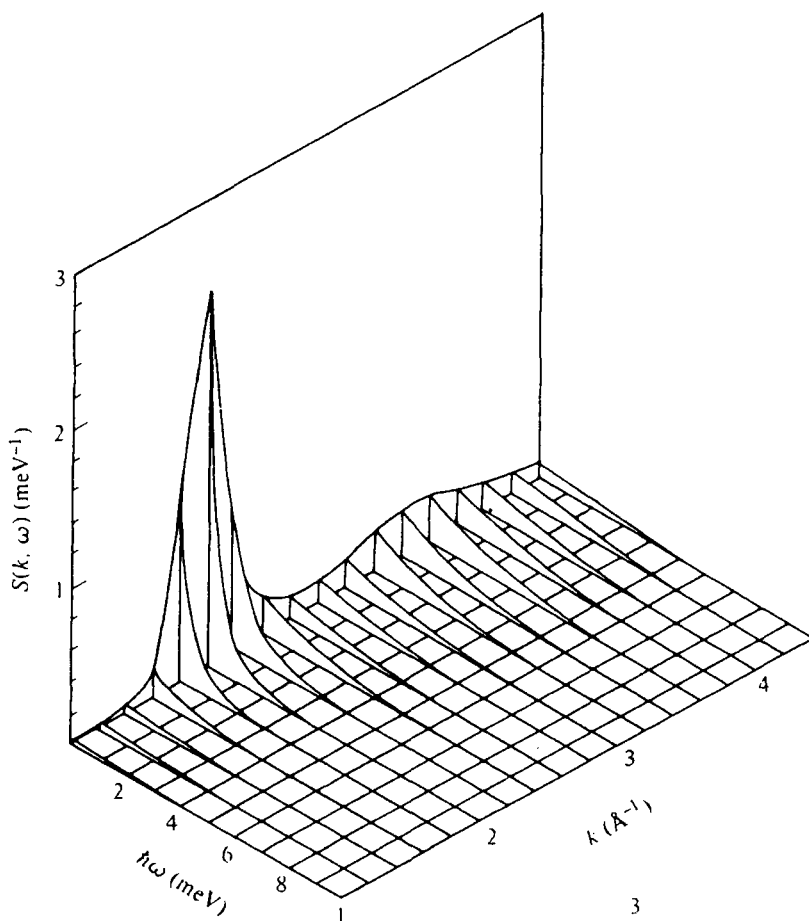
FIGURE 18   The experimentally determined scattering function $S(\kappa, \omega)$ for liquid argon at 85°K for $1 < \kappa < 4.4$ Å showing no signs of side peaks even for the smallest κ-values investigated. Compare theoretical calculations illustrated in Figure 15 lower part (after K. Sköld, J. M. Rowe, G. Ostrowski and P. D. Randolph, 1972).

had neutron absorbing spacers (boron nitride). Temperature 315°K. A careful multiple scattering correction was made. The normalization of data was difficult at small κ-values and was made absolute by comparison to the known second frequency moment. As input in the multiple scattering calculation was used a molecular dynamics calculated scattering function for rubidium. There were also some other difficulties with low energy data: an extra peak which was simply subtracted. The final result is, however, interesting. For the first time true collective high frequency excitations are
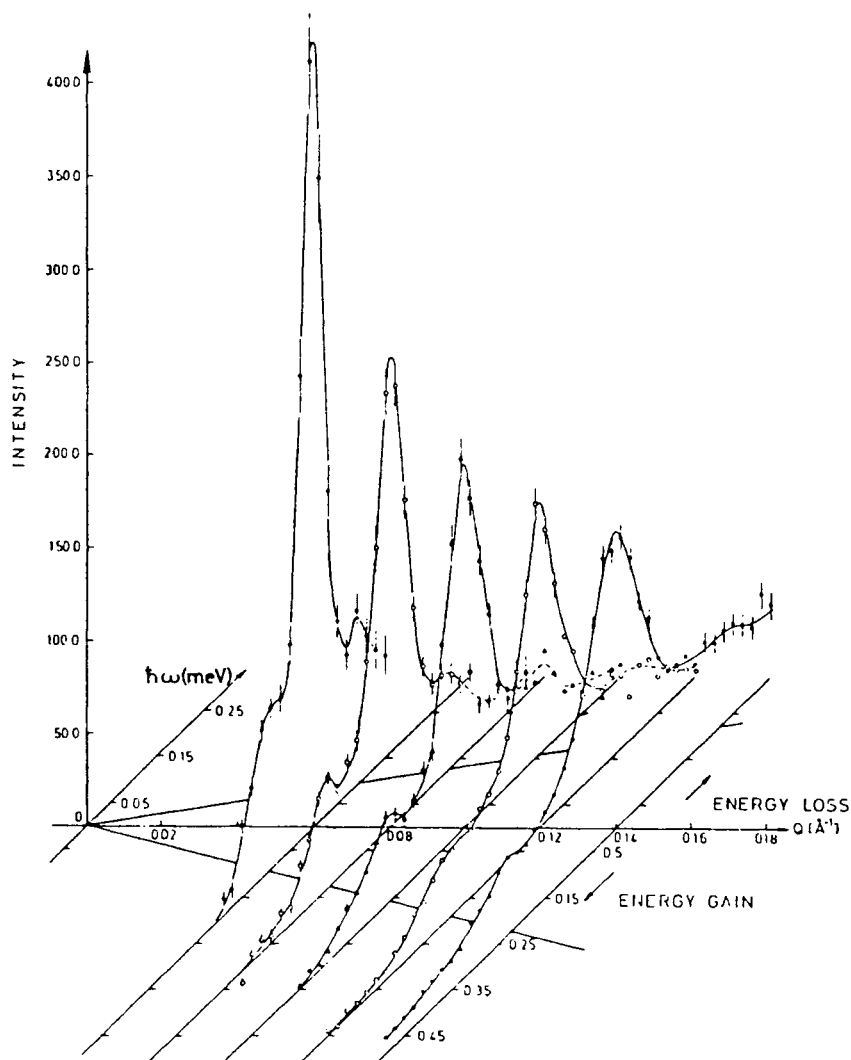
FIGURE 19   Neutron spectra scattered from fluid neon at a density of 0.48 g cm^{-3} at 70°K. Ingoing neutron energy as low as 2.29 and 2.11 meV. Rayleigh and Brilloin peaks are observed for κ < 0.15 Å^{-1}. Compare general similarity with calculations for liquid argon illustrated in figure 15, top part (after B. Bell, H. Moeller-Wenghoffer, A. Kollmar, R. Stockmeyer, T. Springer and H. Stiller, 1975).

observed even at κ-values corresponding to 2/3 of $\kappa_0 = 1.5\ \text{Å}^{-1}$ at which κ-value the main peak of the static structure factor is observed (Figure 20a). This allows a dispersion relation to be traced out (Figure 20b). It indeed shows the structure typical for a solid. It is of interest to notice that $S(\kappa, \omega)$ even in a range $1.25 < \kappa < 2.50\ \text{Å}^{-1}$ shows tendencies to a double structure. Above $\kappa = 3\ \text{Å}^{-1}$ the usual bellshaped structureless form is observed. The structure in the middle κ-region $1.25 < \kappa < 2.50\ \text{Å}^{-1}$ is even better

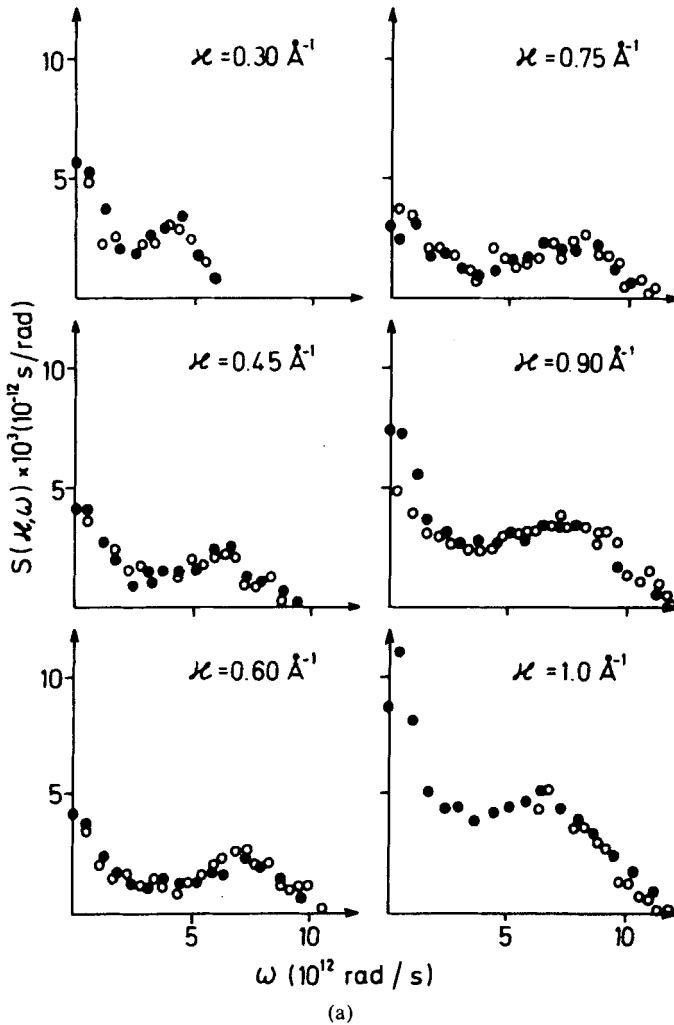(a)

FIGURE 20   a) The experimentally determined scattering function for liquid rubidium at 320°K (melting point at 311.6°K) showing side peaks up to $\kappa = 1\ \text{Å}^{-1}$. Peak of structure factor at $\kappa = 1.5\ \text{Å}^{-1}$.
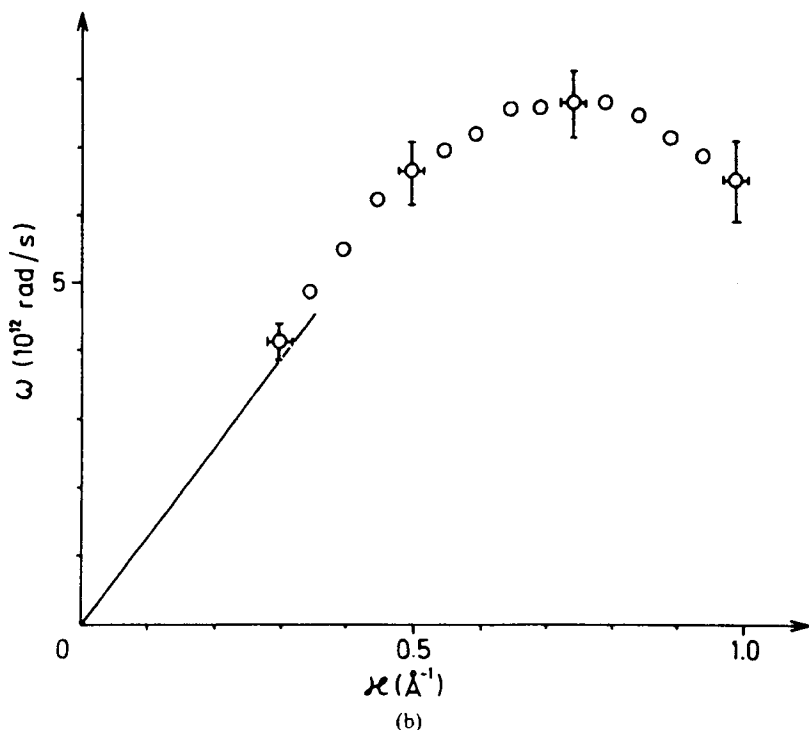
FIGURE 20   b) Dispersion relation $\omega(\kappa)$ for the collective modes of motion given by the side peaks in (a). The solid line corresponds to velocity of sound, c_{ad} ($\omega = c_{ad}\kappa$). Observe that the curve seems to show symmetry round $\kappa_0/2$ (after J. R. D. Copley and J. M. Rowe, 1974).

born out in the shape of the intermediate scattering function. The density-density correlations die out first rapidly and then considerably more slowly, except at $\kappa_0 = 1.5\,\text{Å}^{-1}$, where the same correlations show a very slow decay corresponding to the relatively stable configuration giving the peak at κ_0 (compare Figure 32).

We finally come to the observations performed on liquid lead,[27] $T = 623°\text{K}$. These scattering studies were mainly performed at Studsvik, Sweden, by O. Söderström, but a complementary study was also made at the Laue-Langevin Institute in Grenoble in cooperation between Söderström, Copley, Dorner and Suck. The main mapping of the coherent scattering function at Studsvik was made by use of a time-of-flight spectrometer with 33 and 47 meV ingoing neutron energies. With this combination of energies a mapping for $1 < \kappa < 6.8\,\text{Å}^{-1}$ could be made. In this case $\kappa_0 = 2.2\,\text{Å}^{-1}$. A thinwalled aluminium sample container of plate type was used. Very careful multiple scattering studies were made. The hydrodynamic model of Ailawadi,

Rahman and Zwanzig[23] was used as input scattering function in this calculation. In the studies performed at Grenoble a triple axis crystal spectrometer was used in the constant κ mode of operation. The κ-range covered in this study was $0.4 < \kappa < 1.6\,\text{Å}^{-1}$. Ingoing neutron energy was 40.1 meV. Scattering angles down to 2 degrees could be used in this particular arrangement. The sample container was equipped with gadolinium-containing spacers giving a strong reduction in multiple scattering. No correction for multiple scattering was made in this case mainly because absolute determination of cross section is impossible. The Grenoble studies show again a scattering function with a triple peak structure as in rubidium although the Brillouin peaks are less intense. The features are however visible even above $\kappa_0/2 = 1.1\,\text{Å}^{-1}$ (Figure 21a). From the peak positions it was possible to derive a dispersion relation. But before we present these data we shall compare with the time-of-flight data from Studsvik (Figure 21b). Even in these data a three-peak structure is observed up to about $\kappa \sim 1.3\,\text{Å}^{-1}$ which is above $\kappa_0/2$. The features are still there up to $\kappa = 1.5\,\text{Å}^{-1}$. When these data are combined, a dispersion relation results which extends from $\kappa = 0.3$ to $\kappa = 1.4\,\text{Å}^{-1}$ (Figure 22). These peaks correspond to wavelengths shorter than 20 Å and therefore are outside the hydrodynamic domain. It should however be noted that these peaks are very broad corresponding to a large damping of the corresponding collective excitations. It is also observed that above the main peak in the static structure factor there are no signs of structure in the dynamic structure factor. In passing we notice an important experimental fact. In Figure 21b the dashed lines give the calculated multiple scattering on an absolute scale, the calculation being based on a generalized hydrodynamics model,[23] given in the figure as solid lines. The difficulty to observe the small κ part of $S(\kappa, \omega)$ is illustrated by the increasing importance of the multiple scattering component as the κ-value decreases: the observed peak value of $S(\kappa, \omega)$ for $\omega = 0$ is 0.5 at $\kappa = 2\,\text{Å}^{-1}$ whereas it is only 0.003 at $\kappa = 1\,\text{Å}^{-1}$. The same peak value of the multiple scattering contribution stays approximately constant at 0.02 over this κ-scale.

To sum up, the two investigated insulators show no high frequency collective modes outside the range of validity of normal hydrodynamics whereas the two metals do. Regarding the older attempts to understand the physics of these collective processes the result is meagre. To illustrate the rather dramatic difference between the insulators and metals the region of existence of collective motions and the range of correlations given by $g(r)$ compared to shortest wave length of excitations is given in Figure 23a for neon and 23b for lead.

For larger κ-values the atomic motions should approach free atom motion which is not described by hydrodynamics. Self-motions is in fact approached as κ increases as is visible in $S(\kappa)$. $S(\kappa)$ oscillates round 1 which may be
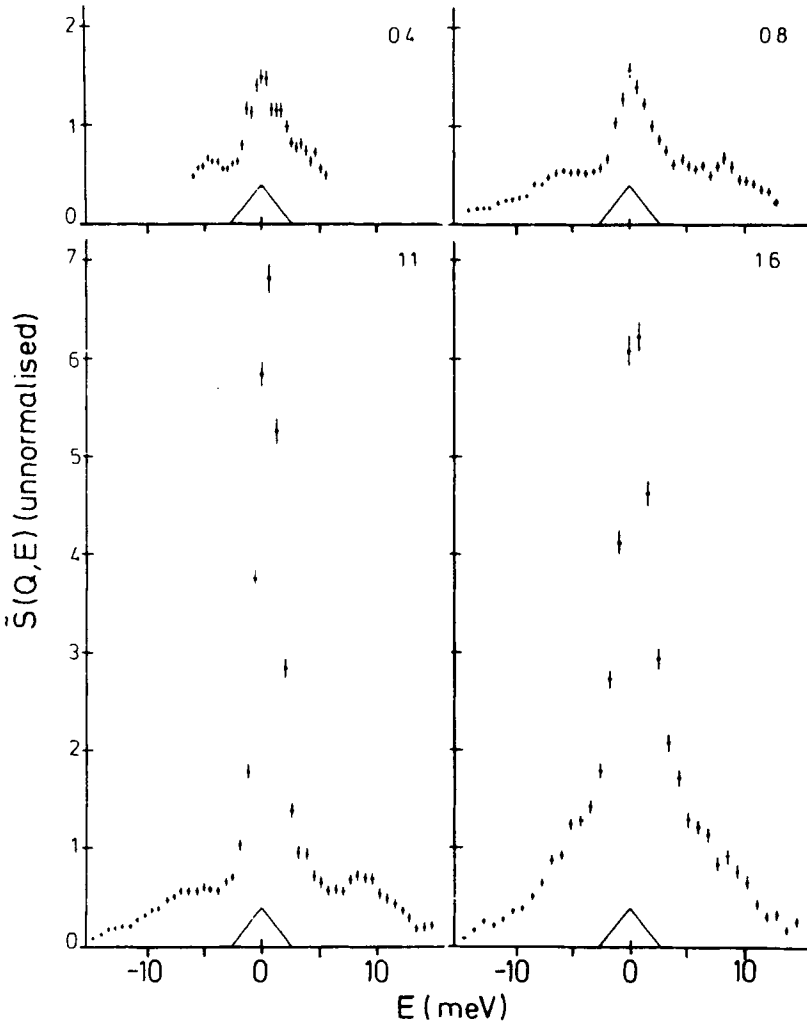
(a)

FIGURE 21   a) Experimentally observed and unnormalized scattering function obtained from liquid lead at 623°K using 40.1 meV ingoing neutron energy in a crystal spectrometer at Grenoble. Sidepeaks are visible at $\kappa = 1.1$, which corresponds to $\kappa_0/2$ (after O. Söderström, J. R. D. Copley, J. B. Suck and B. Dorner, 1980).
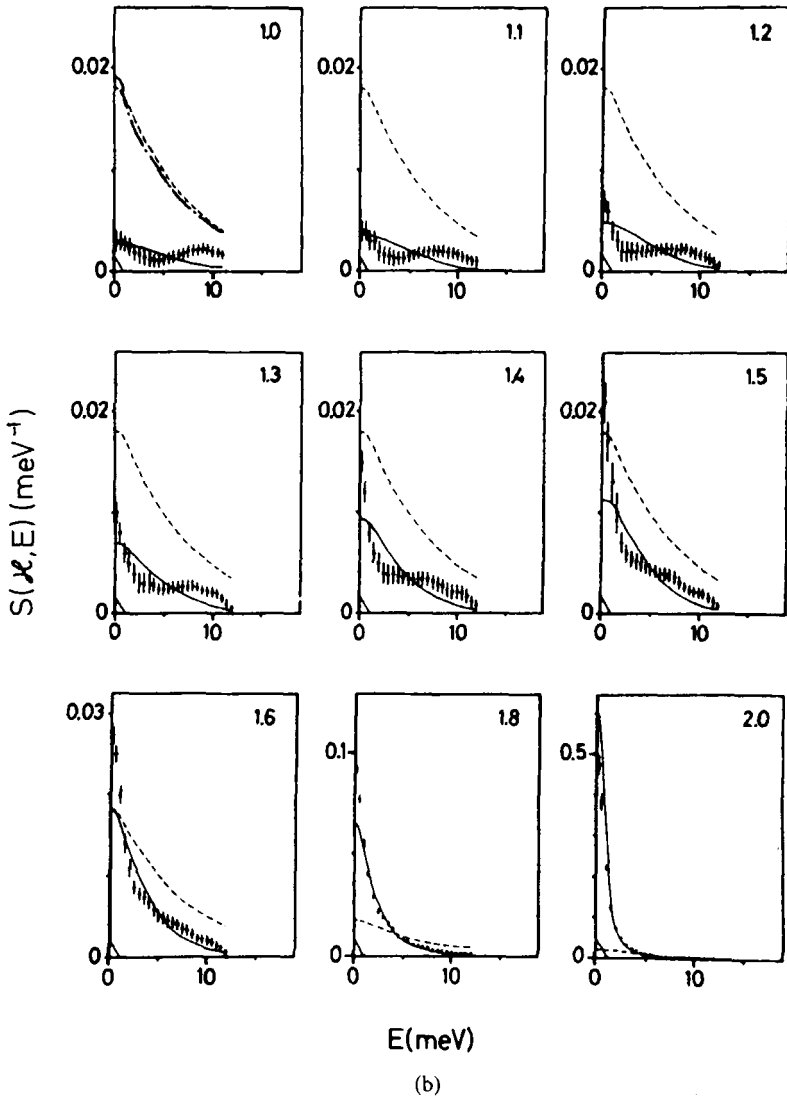
FIGURE 21   b) Experimentally observed and normalized scattering function from liquid lead at 623°K using 33.2 and 47.7 meV ingoing neutron energy in a time-of-flight spectrometer at Studsvik, Sweden. Sidepeaks are visible up to $\kappa = 1.4 \text{ Å}^{-1}$. $(\kappa_0 = 2.2 \text{ Å}^{-1})$. Dashed lines give the multiple scattering contribution (after O. Soderstrom, 1980).
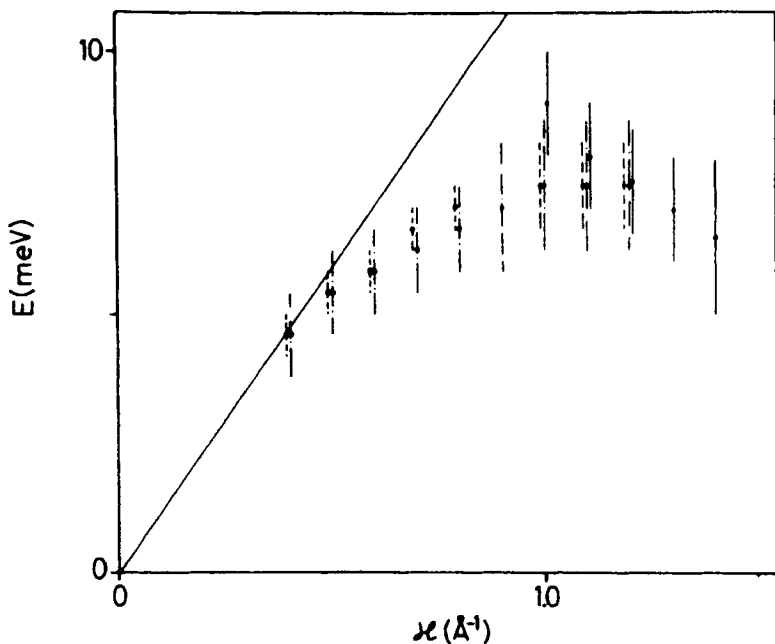
FIGURE 22 Dispersion relation, $\omega(\kappa)$, for liquid lead at 623°K derived from observed side peaks. Also here one notices a tendency for $\omega(\kappa)$ to look symmetric round $\kappa = \kappa_0/2 \, (= 1.1 \, \text{Å}^{-1}$ in the present case). The solid line corresponds to the velocity of sound (after O. Söderström, 1980).
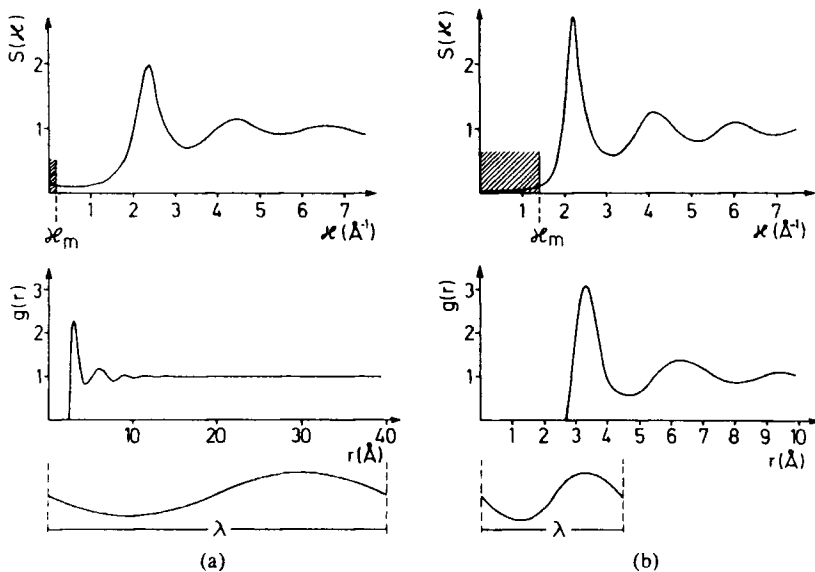
FIGURE 23 The liquid structure factors $S(\kappa)$ and the pair correlation functions $g(r)$ for an insulator, liquid neon, (a) and for a metal liquid lead (b) showing similar gross features. The shortest wave length of collective excitations transmitted over a distance larger than this wave length, $2\pi/\kappa_m$, is however dramatically different being of order $10r_0$ for neon (argon) and of order r_0 for lead (rubidium). Shaded area in $S(\kappa)$ gives region within which excitations are transmitted, r_0 is the position of the main peak of $g(r)$.
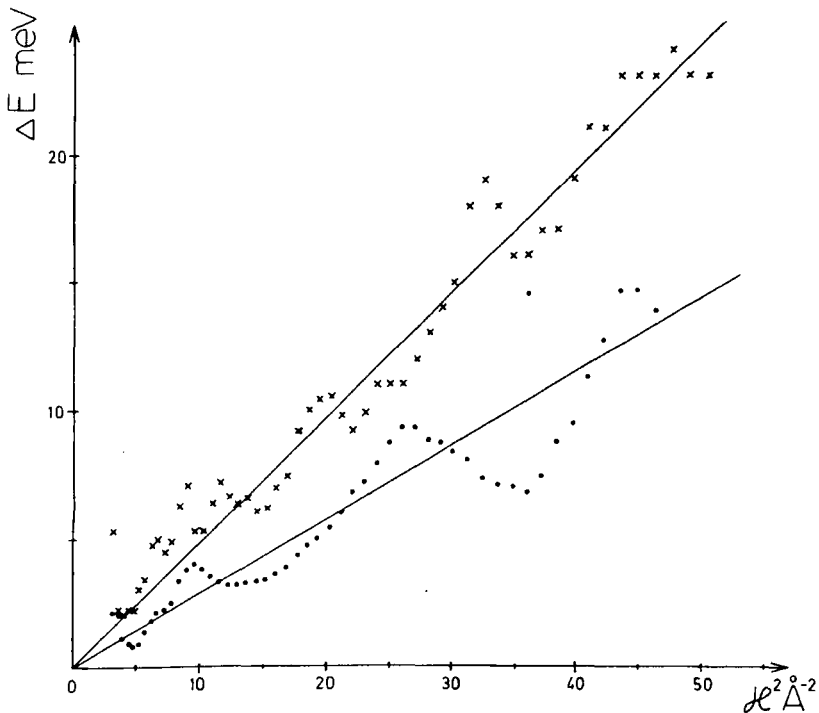
FIGURE 24 Observed full width at half maximum, ΔE meV, of the dynamic scattering function, $S(\kappa, \omega)$, for liquid lead at two temperatures $T = 623°$ ($\circ\circ\circ\circ$) and $T = 1173°K$ (xxxx). The corresponding simple diffusion predictions are given as full lines (after O. Soderstrom, U. Dahlborg, and M. Davidovic, 1982).

considered as the ω-integral of $S_s(\kappa, \omega)$. If one inspects the full width of half maximum (FWHM) of the scattering function it is found that within limits of experimental accuracy of about 10% for lead it oscillates round a half-width value for self motion predicted by simple diffusion[39] (Figure 24). What this picture demonstrates is that when $\kappa > \kappa_0$ the main atomic motion revealed in $S(\kappa, \omega)$ is self motion. The effect mentioned is not too surprising from one point of view namely because simple diffusion is associated with the long time limit or $\omega \to 0$. On the other hand the large κ-values do not go well together with the simple diffusion (Eq. (5) and (6)). The oscillations round $2\hbar D\kappa^2$ may be considered as a kind of corrections to the self motion. What is their nature? What can we learn about the self-diffusion process from such observations? We shall return to these questions in a later chapter.

On the other hand when $\kappa < \kappa_0$ the line width deviates strongly from simple diffusion. This could be expected if that region is considered as a transition region to the low κ-region where true collective excitations exist
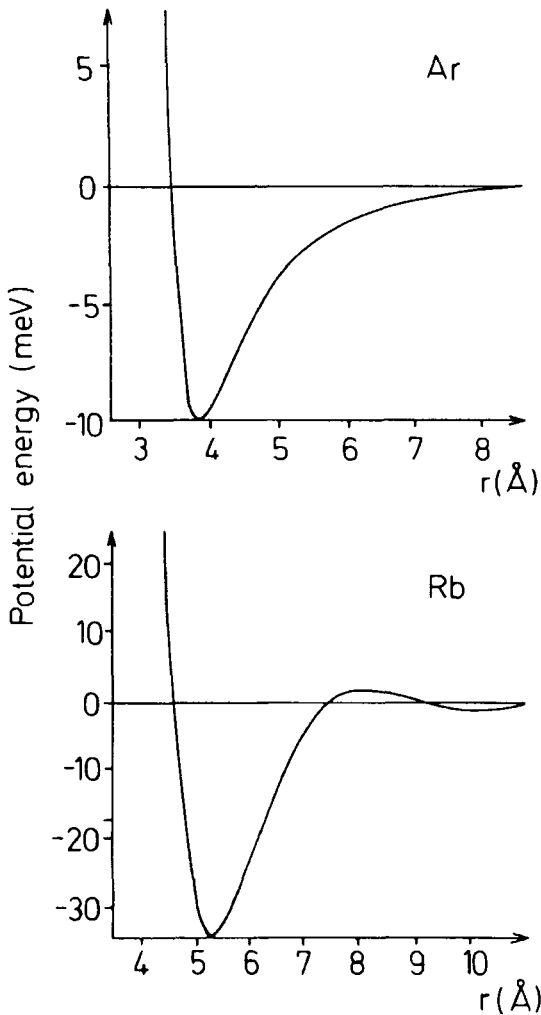
FIGURE 25   Interaction pair potentials for the Lennard–Jones and insulator liquid argon and for the liquid metal rubidium.

in the hydrodynamic sense because these have nothing to do with the self motion. We shall return to these questions later on.

We now have to raise the question: why do we see collective high frequency modes in rubidium and in lead but not in argon and neon. Let us compare the assumed pair potentials acting between for instance argon atoms and rubidium atoms, respectively. The rubidium potential appears more para-bolic and therefore in itself should give rise to some kind of harmonic vibrations (Figure 25). The Lennard–Jones potential is strongly non-parabolic and should give rise to strong anharmonicity, i.e. damping. Also

the shape of the repulsive part varies as $1/r^4$ for rubidium and $1/r^{12}$ for argon. The question is which of these effects are important. Probably both are as we will see in the later part of this analysis.

Molecular dynamics studies by Haan, Mountain, Hsu and Rahman[28] seem to indicate that it is enough to use the repulsive part of the pair potential to reproduce the inelastic peaks in $S(\kappa, \omega)$. They found that they could reproduce the rubidium dispersion relation and also obtained a shorter dispersion region for argon in agreement with earlier results. This seems to indicate that the repulsive core of the potential determines when collective modes can exist. If this limit also determines the limit for hydrodynamics is an open question. The newer kinetic theories shines some light on these problems.

5   Kinetic theories and applications

During the 1970's a new approach to the problem of atomic motions in fluids has been made on the molecular level. This is the kinetic approach in which the problem is attacked from a side earlier used only for low density fluids, where single atomic collision events are dominating. This is a region in which Boltzmanns transport theory is applicable. In the early 1920's Enskog at the Royal Institute of Technology in Stockholm succeeded in extending the validity of Boltzmanns theory to moderately dense gases. But still in Enskogs theory the velocity auto correlation function decays exponentially as in simple Langevin diffusion. It has been shown that to come further along these lines one has to consider the possible recollisions of atoms. Such recollisions change in nature with the density. This was shown in a famous molecular dynamics study by Alder, Gass and Wainwright[15] 1970. It was also shown by these research workers and others that $\langle v_x(0)v_x(t)\rangle$ for long times decays as $t^{-3/2}$ and not as an exponential. The reason for the deviation from the Enskog behaviour at lower densities is the so called ring collisions, let us say of smoke ring type. At higher densities and shorter wave lengths the cage effect is dominating. In kinetic theory it is natural to start out from the binary collision and to try to include corrections involving the recollision effects.

The development of kinetic theory[29] for a dense medium is by nature very complex as not only two particle correlations but also higher order correlations must be considered.† The full phase space distribution function is considered and the fluctuations in the form of deviations from the mean, which

---

† As a good example of what can be achieved by use of kinetic theory for a dense fluid the series of papers published by Sjögren and Sjölander[29,30] is mentioned here. Particularly the last series of papers[29] on kinetic theory of self-motion in monoatomic liquids and the corresponding paper on kinetic theory of current fluctuations in simple classical liquids with numerical results are of importance in the present connection.

is the equilibrium distribution, are defined. The equations of motion for the correlations between deviations at different phase space points are set up.

The complicated collision integrals that always enter a Boltzmann equation type of treatment occurs also here but the form of the equations is recast such that all the complicated couplings between various modes of motion are combined into a memory function in the Mori type of formalism. If this memory function can be calculated, then for instance the self motion and therefore $S_s(\kappa, \omega)$ can be described.

Also for the pair correlation function has it been possible to derive a similar memory function. It turns out that the scattering function in this kinetic approximation contains terms which can be identified as corrections to the lower approximation theories produced earlier. If we set the convolution approximation as the first one, then the mean field approximation is the second and the kinetic theory is the third. The kinetic theory gives the correct hydrodynamic limits for transport functions and also the right short time limit namely the free gas model (Eq. 8). It also turns out that the self motion plays a very important role in both the final expression for the coherent scattering function directly and in the many mode coupling integrals that appear in the memory function. A particularly important role is played by the part of the memory function that describes the binary collision: this was expected as this is the primary driving agent in the dynamical process. So far a theoretical description of the binary collision event is missing. As the slower decaying part of the memory function is found to start out as t^4, it is argued that the faster decaying part connected to terms of order t^2 may be approximated by a Gaussian ansatz $\exp|-t^2/\tau^2(\kappa)|$. But as distinguished from for instance the ansatz for the memory function used in the framework of generalized hydrodynamics mentioned earlier, the parameter $\tau(\kappa)$ is not guessed. It is determined from an expansion of the exact formal expression of the memory function. It is instructive to know that the memory function can be expressed as $\Gamma(z) = \Gamma^B(z) + \Gamma^R(z)$ where the first part describes the rapidly decaying memory due to the fast binary collisions and the second part contains the intermediate and long time recollisions of ring type. Hydrodynamic modes are connected to intermediate and long times. Instead of making a self consistent calculation of a scattering function one assumes reasonable approximate expressions for the various coupling integrals containing the correlation functions $F_s(\kappa, t)$, $F(\kappa, t)$, $C_l(\kappa, t)$ and $C_t(\kappa, t)$ which are the only correlation functions that are considered. $F_s(\kappa, t)$ and $F(\kappa, t)$ are intermediate scattering functions of $S_s(\kappa, \omega)$ and $S(\kappa, \omega)$, whereas $C_l(\kappa, t)$ and $C_t(\kappa, t)$ are the intermediate expressions for longitudinal and transverse current correlation functions.

The crucial parameter in shaping the steep part $\Gamma^B(z)$ of the memory function is the relaxation time $\tau(\kappa)$ similar for self motion and pair motion.

It contains the effects of the static structure round any atom such that a simple binary collision between two particles in a vacuum interacting with the bare potential is renormalized due to presence of neighbours in the given *static* configuration. This decreases the value of τ^{-2} in the present kinetic theory by some 35%. As seen from the Figures 26a and b a further decrease of τ^{-2} by some 25% resulting in a slight broadening of $\Gamma^B(t)$ is enough to create an almost perfect agreement between the calculated velocity auto correlation function and the computed one using molecular dynamics. The authors[29] (Sjogren in J. Phys. C, **13**, (1980)) believe that in this phenomenological way they have taken the other *rapid dynamical* renormalizations into account. So with other words: as a result of a binary collision a certain number of near neighours undergo rapid replacements. *This rapid adjustment to the new situation amongst very near neighbours may be thought of as being produced by both repulsive and attractive forces.* This conclusion may be drawn from a comparison of Sjögrens results described above with the velocity auto correlations computed by Haan, Mountain, Hsu and Rahman[28] cited above. As seen from their results for rubidium (Figure 27b) concerning the velocity auto correlation function obtained with only the repulsive part of the potential active (full curve) and the one obtained using the full potential (dashed curve), the difference between the two is just of the same nature as obtained by Sjögren from the small adjustment of the binary collision part of the memory function (Figure 27a). The rapid readjustments of near neighbours has a clear effect on vital parts of the velocity auto correlation function creating more pronounced oscillations — or if we like to use an old-fashioned language — creating a more solid-like behaviour.

The long tail of $\Gamma(t)$, $\Gamma^R(t)$, is created by effects of coupling between self motion and density fluctuations, self motion and transversal and longitudinal currents, respectively.

Theoretical results similar to the one for liquid rubidium described above were obtained for liquid argon. It is, however, apparent that agreement between kinetic theory prediction and molecular dynamics results is not quite so perfect for argon. Sjögren[29] speculated that the origin of this disagreement may be the steep part of the potential. In the case of argon it falls off as r^{-12} and it could be expected that the pair collision is more violent. In such a case the reaction back on the surrounding may be stronger such that additional modes should have to be included in the description of the couplings.

To demonstrate to what degree the kinetic theory in the present state of development is able to describe the physics of the short wave length "Brillouin peaks" in a metal we consider the case of liquid rubidium. This was the first case for which such collective modes were observed in neutron scattering. Furthermore a molecular dynamics calculation also exists which may be
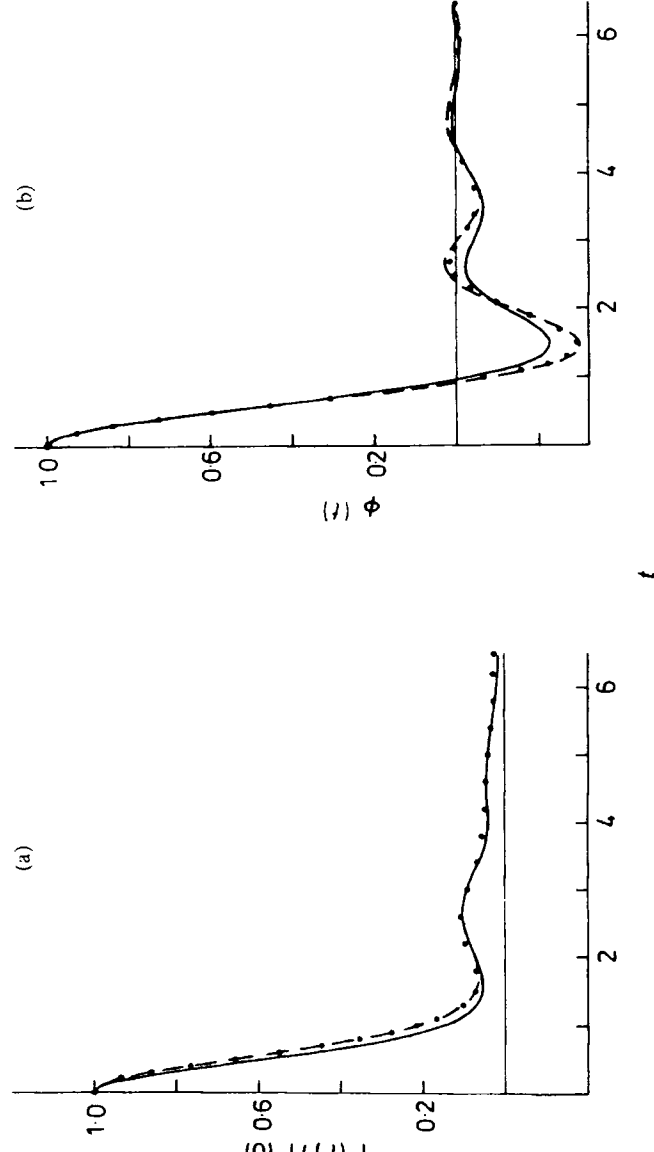
FIGURE 26 a) Normalized memory function for self motion in liquid rubidium. Kinetic theory (——) and molecular dynamics results of Rahman (....). (----) shows kinetic theory adjusted to agree with molecular dynamics. Observe that the adjustment affects only the binary collision part Γ^B. b) Normalized velocity correlation function for rubidium. Same symbols as in (a). Unit of time is 3.212×10^{-13} s (after L. Sjogren, 1980).
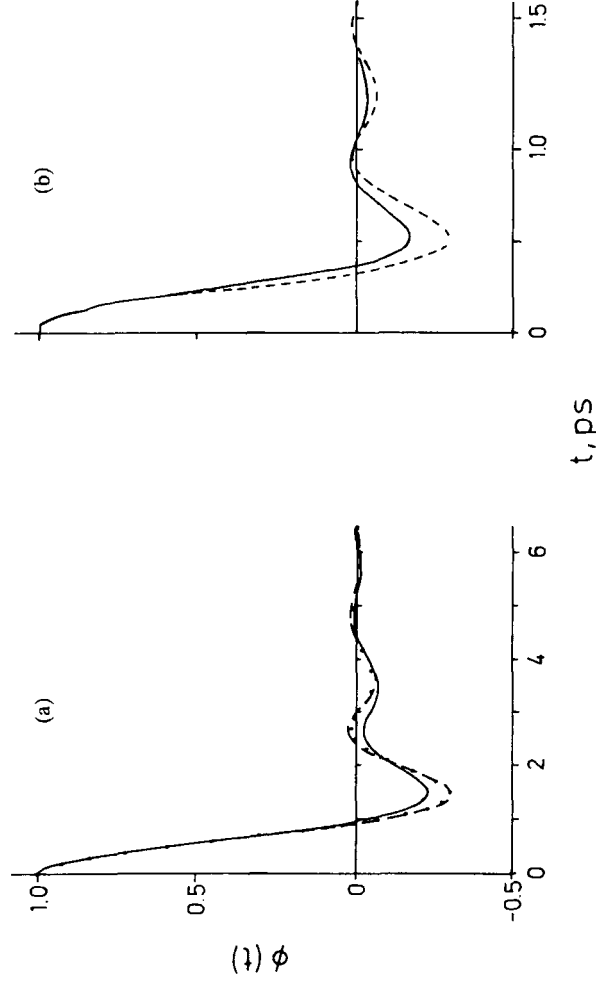
FIGURE 27   a) Velocity correlation function for liquid rubidium assuming bare pair collision with due consideration of static atomic arrangement round the collision site (———) and with consideration also of the rapid dynamic adjustments of atoms near the collision site (- - -). (. . . .) molecular dynamics result of Rahman (after L. Sjogren, 1980). b) Velocity correlation function for liquid rubidium assuming only repulsive part of pair potential active (———) and assuming the full potential active (- - - -) (after S. W. Haan, R. D. Mountain, C. S. Hsu and A. Rahman, 1980).

FIGURE 28   Dynamic scattering function $S(\kappa, \omega)$ versus ω calculated from kinetic theory and molecular dynamics ($\cdot\cdot\cdot$). a) (- - - -) only binary collisions included in memory functions. ($:\ldots$) gives scattering function when also certain ring collision te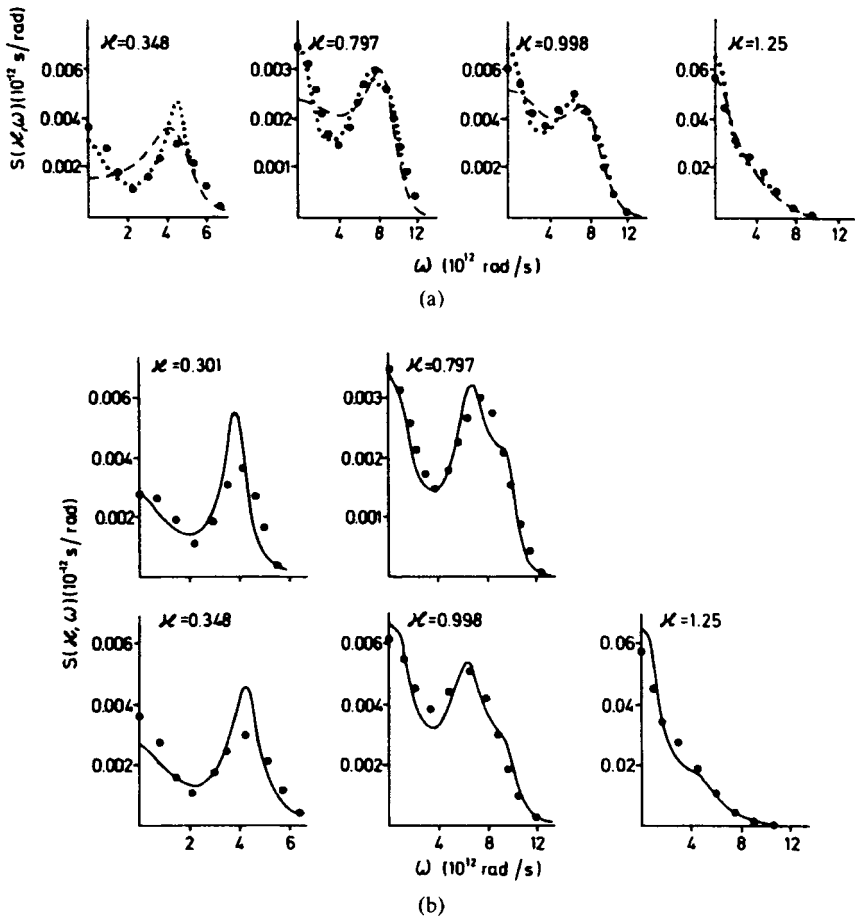rms describing coupling between self-motion and density fluctuations are included. b) (———) gives final kinetic theory prediction when all coupling terms are included in the ring collision part of the memory function (after L. Sjögren, 1980).

used for comparison with theory. Including various components of the memory functions $\Gamma(z)$ for self motion and $\Gamma_d(z)$ for the pair motion, Sjögren[29] was able to show quite clearly how the various features of the observed or computed $S(\kappa, \omega)$ are built up (Figure 28a). It is of interest to notice that if only the binary part $\Gamma^B(t)$ is included the inelastic features identified as Brillouin peaks are observed. This observation is in accord with the computations of Haan, Mountain Hsu and Rahman[28] that the repulsive part of the potential plays a dominant role. It should further be noticed that the wave

length of these excitations is in a range determined by $0.3 < \kappa < 1.25 \text{ Å}^{-1}$. The value of $\kappa_0/2$ is 0.75 Å^{-1}. Already when the coupling to density modes is introduced the scattering function is rather well described. When all the terms in the present approximation are included the theoretical reproduction of molecular dynamics or measured data is even quantitatively good (Figure 28b).

The real reason why short wave length excitations are absent in argon or neon, Brillouin peaks being observed only up to 0.2 á 0.3 Å^{-1}, compared to $\kappa_0/2 \cong 1 \text{ Å}^{-1}$, is not yet demonstrated clearly. One may speculate that the combined effect of the hard repulsive core and the strongly anharmonic form of the potential well in the Lennard–Jones case is the reason. The molecular dynamics results indicate such a conclusion.

It is appropriate to state here that the physical guesses performed by the early model builders in this field, such as Singwi as discussed above, as a matter of fact came quite close to what modern sophisticated kinetic theory has found. Round each atom there probably is a little sphere of coherence of radius a very few atomic distances within which very rapid readjustments occur giving rise to collective motions of a nature not very different from the situation prevailing in a solid. The difference is that there is not periodic structure in the liquid which can carry a true phonon-like excitation over longer distances. This will be damped out and become aperiodic for those κ-values where the disordered structure is resolved and dominating, i.e. $\kappa > \kappa_0/2$ in the metals investigated so far. The detailed value of κ where the collective mode is damped out probably depends upon potential shape.

6 New interpretation of old data

As discussed in the first chapter of this review the measurements with cold neutron inelastic scattering on liquid aluminium and other substances, which triggered the new thinking in the field of microscopic theory of liquids, seemed to indicate that the scattered spectrum from a solid polycrystalline high temperature sample looked similar to the one scattered from a liquid sample (Figure 7b). Now we have seen other more complete studies on liquid metals such as those on rubidium and lead from which it seems clear that propagating collective density fluctuations do not exist in these metals above a κ-value of about $2/3\kappa_0$. On the other hand in a solid phonons — although strongly damped — were shown to exist up to the melting point. In order to understand the old study a more careful analysis has to be made.[31]

First let us ask for the κ-values at which the measurements were made. As all time-of-flight studies these were constant angle observations so that both κ and $\Delta\omega$ varies along the observation curve in the κ-$\Delta\omega$ plane (here $\Delta\omega$ is used for energy transfer and ω to indicate the running energy scale). It is

found that the κ- and $\Delta\omega$-ranges covered for aluminium at the constant scattering angle of 60° are $1.7 < \kappa < 7\,\text{Å}^{-1}$ and $1 < \omega < 14 \times 10^{13}\text{rad/s}$. The important κ- (or, equivalently, wave length-) domain ranges from slightly below $\kappa_0 = 2.7\,\text{Å}^{-1}$ to high values. Large energy changes are mostly observed. We have seen earlier that in corresponding domain the observed scattering functions in rubidium and lead are simply very structureless and continuously decaying. But along the loci of observation for aluminium the κ-value varies and we have to look closer into the structural effects, i.e. the topology of $S(\kappa, \omega)$.

Fortunately $S(\kappa, \Delta\omega)$ was determined for liquid aluminium in a molecular dynamics study by Ebbsjö, Kinell and Waller[32] and it was also calculated on the basis of the Sjögren-Sjölander theory such that both $S(\kappa, \Delta\omega)$ and $S_s(\kappa, \Delta\omega)$ as well as $S(\kappa)$ were known.[33] This means they are known on the basis of the assumed pair potential acting between the atoms. Various such potentials were tried by Ebbsjo, Kinell and Waller and they applied them to a calculation of the dispersion relation of phonons in low temperature aluminium from which was learnt that even very different potentials give similar predictions of dispersion relations. Also the scattering functions derived from the molecular dynamics studies using three different potentials show that propagating collective motions in aluminium are probably damped out at κ-values $< 2/3\kappa_0$. What is then the message of the old measurements?

In order to solve the problem two steps were taken. First a more reliable multiple scattering calculation was made using the molecular dynamics data as a scattering kernel. Then this multiple scattering was added to the scattering function calculated by Sjögren ($\sim$ the molecular dynamics study data). Observe that the *multiple scattering is added to the theoretical model. The experimental data are left untouched.* The calculated compounded spectrum was compared to observation. The agreement was quite reasonable.[31]

But how can the liquid spectrum be similar to the polycrystalline one? To get an answer to this question we have to look into the topology of $S(\kappa, \Delta\omega)$ and into the kinematics of the experiment. It is known that what one measures directly in a time-of-flight experiment is not $S(\kappa, \Delta\omega)$ but rather something proportional to $\omega^2 S(\kappa, \Delta\omega)$. It is therefore instructive to plot the theoretical $S(\kappa, \Delta\omega)$ and $\omega^2 S(\kappa, \Delta\omega)$ in a three-dimensional plot along the locus for the 60° angle of observation (Figure 29). It is seen that exactly the double peaked structure observed in the scattered neutron spectra is produced: the first peak due to the liquid structure factor $S(\kappa)$ and the second peak being a time-of-flight artifact.

However, in order to understand the physics behind the similarity of the two spectra from polycrystal and liquid, one has to make a theoretical
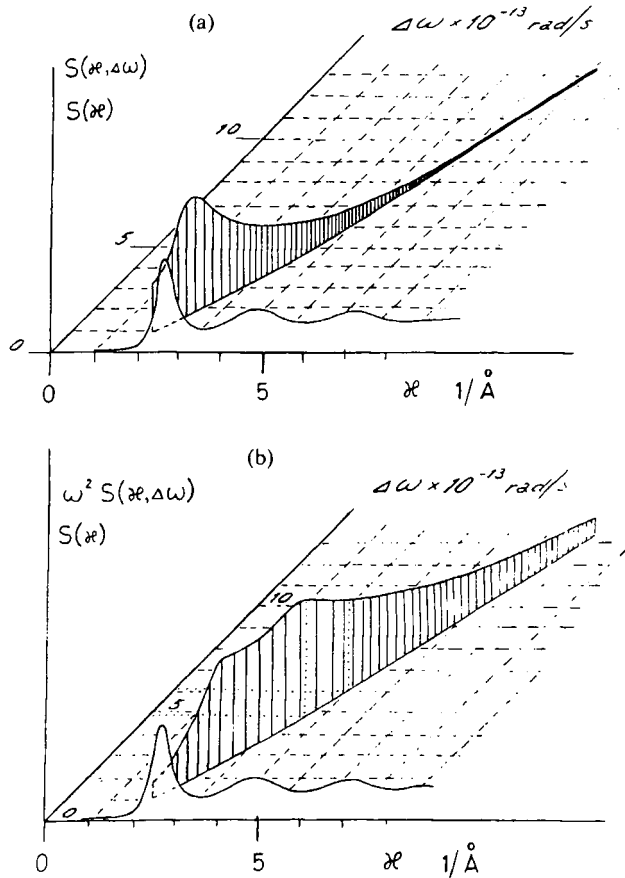
FIGURE 29 a) Value of scattering function, $S(\kappa, \Delta\kappa)$, for liquid aluminium 950°K from kinetic theory along the locus of the 60° angle of observation for beryllium filtered ingoing neutrons. Shown is also the structure factor for liquid aluminium. b) Value of $\omega^2 S(\kappa, \Delta\omega)$, which is the quantity observed in a time-of-flight experiment, for liquid aluminium. Shown is also the liquid structure factor (after K. E. Larsson, 1980).

analysis and penetrate deeper. We have already seen that during the development of theoretical ideas for liquid dynamics three models were stepwise adding new and higher approximations to the previous one namely 1) the convolution approximation, 2) the mean field approximation and 3) the kinetic theory.

The scattering function from these three approximations was calculated, Kerrs expression[34] for the mean field case being used and the last one being taken from Sjögrens computations,[33] and compared to the experimental result at 60° angle from 1959. With the kinetic model data normalized to one
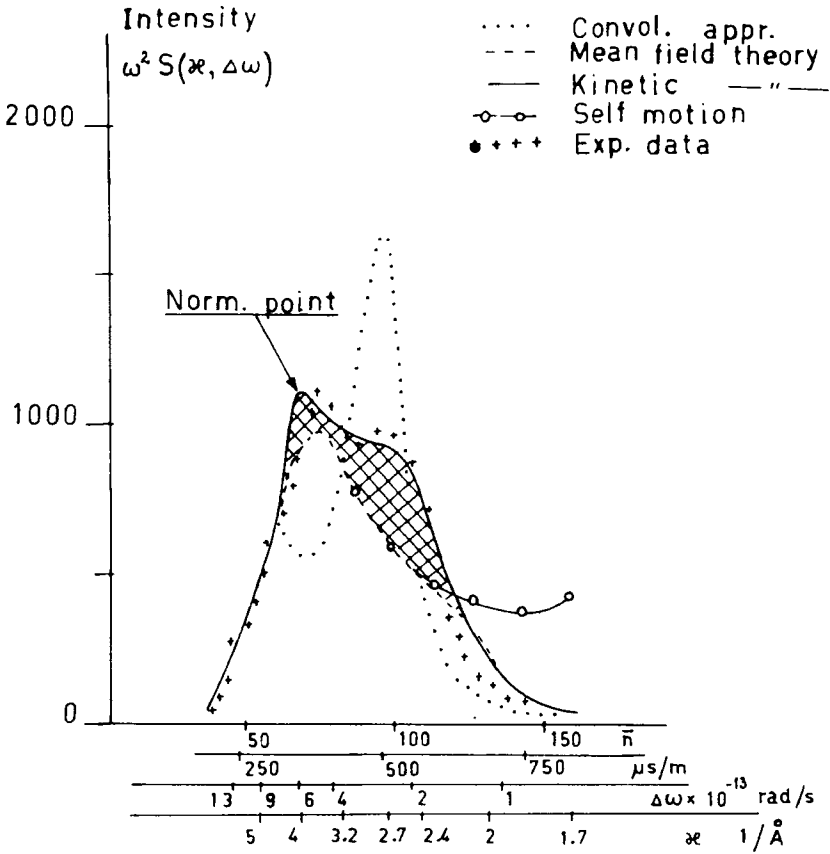
FIGURE 30 Calculated values of $\omega^2 \, S(\kappa, \omega\Delta)$ for liquid aluminium corresponding to 60° angle of observation based on three different degrees of theoretical approximation: convolution approximation (. . . .), mean field approximation (- - - -) and kinetic theory (———) compared to experimental results (+ + + +). Shown is also the value of $\omega^2 \, S_s(\kappa, \Delta\omega)$, which describes self motion and corresponds to incoherent scattering. The theoretical models are given on a correct scale relative to each other but the kinetic theory is normalized to one point (after K. E. Larsson, 1980).

experimental point the total result shows (Figure 30) that in fact the various approximations describe data better with increasing degree of sophistication.

In order to further analyze the results from the three theoretical models it is profitable to slightly reformulate the expressions for the scattering functions, $S(\kappa, \Delta\omega) = 1/\pi \, \mathrm{Re} \, F(\kappa, z = i\Delta\omega)$, in the following way.
The convolution approximation is:

$$F(\kappa, z)_1 = S(\kappa)F_s(\kappa, z). \tag{22}$$

The mean field approximation[34] is:

$$F(\kappa, z)_2 = F(\kappa, z)_1 - C_1(\kappa, z) \qquad (23)$$

The kinetic theory in the present approximation (slightly approximated):

$$F(\kappa, z)_3 \simeq F(\kappa, z)_1 - C_1(\kappa, z) - C_2(\kappa, z) \qquad (24)$$

The functions $C_1(\kappa, z)$ and $C_2(\kappa, z)$ may be considered as correction terms. The first, $C_1(\kappa, z)$, which brings the convolution to the mean field approximation, is to a large degree determined by the static structure factor via the direct correlation function. It is a characteristic approximation in mean field theory to replace the bare atomic interaction with an average one represented by the direct correlation function. There is no distinguished role played by a binary collision as driving agent. The second, $C_2(\kappa, z)$ which brings the mean field approximation into the kinetic theory approximation contains as a dominating term the memory function $\Gamma^d(\kappa, z)$ for pair motion. A closer inspection of the various formulas reveals the important role played by the self motion via $S_s(\kappa, \Delta\omega)$. As seen in Figure 30 the collective effects die out very quickly in the mean field approximation for $\Delta\omega > 2 \cdot 10^{13}$ rad/s and $\kappa > 2 \, \text{Å}^{-1}$ such that $S(\kappa, \Delta\omega)_{\text{mean field}} \rightarrow S_s(\kappa, \Delta\omega)$. This is equivalent to stating that $C_1(\kappa, z) \rightarrow F_s(\kappa, z)[S(\kappa) - 1]$ under these conditions. Therefore the scattering function in the highest approximation, the kinetic, is mainly determined by

$$F(\kappa, z)_3 = S(\kappa)F_s(\kappa, z) - F_s(\kappa, z)(S(\kappa) - 1) + C_2(\kappa, z) = F_s(\kappa, z) - C_2(\kappa, z).$$

We remember that $C_2(\kappa, z)$ is dominated by the memory function $\Gamma^d(\kappa, z)$ for pair motion. In a separate study Sjödin and Sjölander[35] have shown that for $\kappa > \kappa_0$ the memory function Γ^d reduces to $\Gamma^{d,B}$, its binary collision dominated short time behaviour part, represented in the present approximation with a Gaussian function of width $\tau(\kappa)$. We remember from the latest study of the memory function by Sjögren[29] discussed in the previous chapter that the simple two body binary collision has to be corrected slightly to include other rapid processes in the medium near the self particle. This is then the only effect of "damped phonons" that is left in the liquid. To further expose the difference between the mean field and the kinetic approximations one might plot the factors $S(\kappa, \Delta\omega)_{\text{mean field}}/S_s(\kappa, \Delta\omega) = f(\kappa, \Delta\omega)$ and $S(\kappa, \Delta\omega)_{\text{kin, th}}/S_s(\kappa, \Delta\omega) = g(\kappa, \Delta\omega)$ in a three dimensional plot (Figure 31). It is seen that the collective effects in the kinetic case show up as oscillations in $\Delta\omega$ and extend further out in $\Delta\omega$. But the effects are only small corrections to $S_s(\kappa, \Delta\omega)$ for the present case that $\kappa > \kappa_0$. As we have seen in earlier chapters the situation is altogether different when $\kappa < \kappa_0$. The collective phenomena then tend to dominate, which corresponds to the fact that $S(\kappa) \ll 1$ such that $S(\kappa, \Delta\omega)$ is widely different from $S_s(\kappa, \Delta\omega)$. The reason
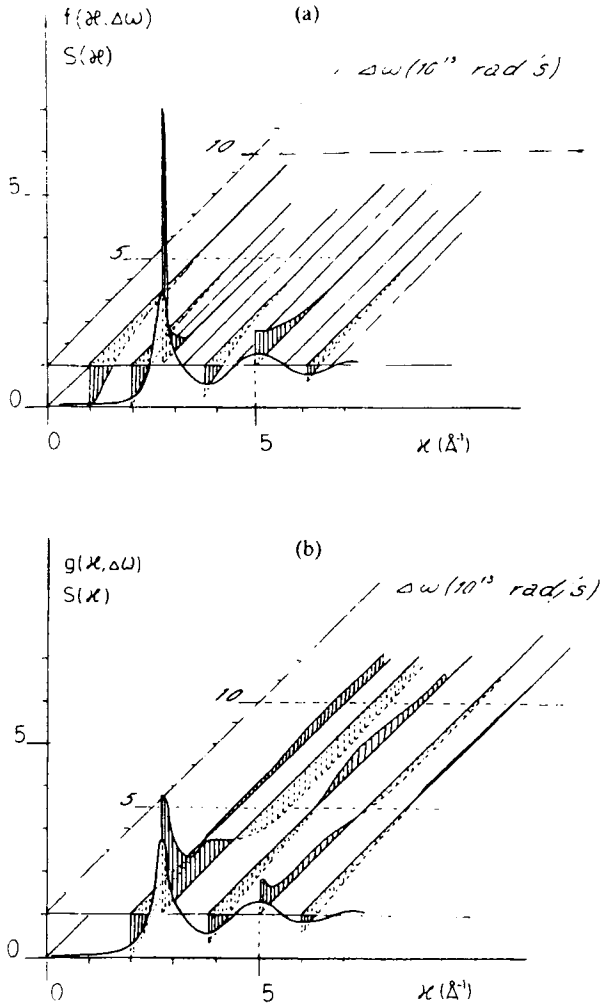
FIGURE 31   Ratio $S(\kappa, \omega\Delta)/S_s(\kappa, \omega\Delta)$ for liquid aluminium. $S_s(\kappa, \omega\Delta)$ is obtained in the gaussian approximation, Eq. (4), and using Eq. (12) to calculate $\overline{x^2(t)}$. The velocity correlation function is obtained from a molecular dynamics study.[32] $S(\kappa, \omega\Delta)$ is calculated (a) on the basis of mean field theory (ratio $= f(\kappa, \omega\Delta)$) and (b) on kinetic theory (ratio $= g(\kappa, \omega\Delta)$). Shown is also the appropriate liquid structure factor (after K. E. Larsson, 1980).

that $S(\kappa) \ll 1$ is that

$$S(\kappa) = \int_{-\infty}^{+\infty} S(\kappa, \Delta\omega)\, d(\Delta\omega) = \int_{-\infty}^{+\infty} S_d(\kappa, \Delta\omega)\, d(\Delta\omega)$$

$$+ \int_{-\infty}^{+\infty} S_s(\kappa, \Delta\omega)\, d(\Delta\omega)$$

in which the two last terms almost cancel each other for $\kappa < \kappa_0$.

It is easy to show that there exists a strong similarity between this modern and very complex theory and the old phenomenological model by Singwi. We remember that Singwi assumed that round each atom in a liquid there is a range of coherence, R, within which elastic vibrations occur for a very short time, $< 10^{-12}$s; outside this range diffusion guided by the liquid static structure occurs. In mathematical shape this prediction of scattering function very much looks like the one derived above from kinetic theory. Both forms contains a correction factor to the convolution approximation. It may be shown that the two correction terms related to $H(\kappa, \omega)$ in Eq. (11) and $C_2(\kappa, z)$ in Eq. (24) are of the same shape if a R-value is selected that best describes data.[31] The two ideas contain similar physics. The R-value giving best fit is 17 Å indicating that quite a few neighbours to the central atom should be engaged in a coherent motion. But clearly at these short wave lengths—large κ-values—the damping due to static disorder is so strong that no inelastic peaks are formed in $S(\kappa, \Delta\omega)$.

The fact that $S_s(\kappa, \omega)$ (here ω is again used instead of $\Delta\omega$ for energy transfer) plays a central role for $\kappa < \kappa_0$ is displayed in many ways. The FWHM is found to oscillate round $2\hbar D\kappa^2$ at least for lead and neraly so for argon[40] (Figure 24). The structure factor $S(\kappa)$ oscillates round one (1). The fact that the FWHM of $S(\kappa, \omega)$ oscillates round a half width value of $S_s(\kappa, \omega)$ accurately given by the simple diffusion expression in the case of lead must mean that in this case the phenomenon of self-diffusion is defined down to the very small wave lengths involved $\lambda \sim 2\pi/\kappa \sim 1$ Å. Now the self diffusion coefficient may be defined by

$$D(\kappa) = \frac{k_B T}{M \int_0^\infty \Gamma^s(\kappa, t)\, dt} \tag{25}$$

Here the diffusion coefficient is considered a transport function (wave length dependent). The fact that FWHM oscillates round $2\hbar D\kappa^2$ with a *constant* value of D corresponding to its long wave length (static) value and shows no experimentally observable tendencies to deviate from it must mean, that the time integral over the memory function $\Gamma^s(\kappa, t)$ is κ-independent within experimental error. The large absolute values of the widths observed at $\kappa \sim 6$ Å^{-1}, which are of order 7 meV for lead, indicate that the main part

of the integral is performed for $t = \tau \sim 6 \cdot 10^{-13}$s. Here we have invoked the relation that $v\tau$ should be of order one. As the diffusion constant is defined only for the long time limit, in principle, $t \to \infty$ or $\omega \to 0$ this observation means that the main part of the time integral is obtained already after a short time of order $6 \cdot 10^{-13}$s for the case that $\kappa > \kappa_0$. It appears as if the intermediate time behaviour of $\Gamma(t)$ (ring collision) is of little importance as well as the long time behaviour leading to the well known $t^{-3/2}$-behaviour of $\langle v_x(0)v_x(t)\rangle$ in this large κ domain. It is the rapidly decaying part of $\Gamma(t)$ which is the dominating factor in building up the diffusion constant. If we think of D as defined from Einsteins relation $\overline{x^2} = 2Dt$ we are led to the conclusion that this long time asymptotic formula is valid down to distances of order 1 Å and times of order $6 \cdot 10^{-13}$s.

In the case of liquid rubidium the observed FWHM deviates considerably from the simple diffusion expression. As shown by molecular dynamics calculations[36,37] the FWHM of $S_s(\kappa, \omega)$ oscillates round the simple diffusion value with a rather large positive deviation from $2\hbar D\kappa^2$ just at κ-values round 3–5 Å^{-1}. If this is taken into account it is found that again the observed FWHM of $S(\kappa, \omega)$ oscillates round the FWHM of $S_s(\kappa, \omega)$.[40] So again we see the leading role of $S_s(\kappa, \omega)$ demonstrated. The origin of the large deviation of the FWHM of $S_s(\kappa, \omega)$ from $2\hbar D\kappa^2$ has been shown[37] to be the dominant role played by binary collision effects which are large in this case. In the case of liquid argon a similar phenomenon has been observed but of smaller magnitude.[36,17]

We have thus seen that for $\kappa < \kappa_0$ the neutron scattering results on the four liquids argon, neon, rubidium and lead have shown us to what degree collective excitations of the nature observed in the form of Brillouin peaks exists. For $\kappa > \kappa_0$ the observations have shown the collective behaviour to appear more or less as a minor correction to self motion. Consequently from this κ-range we may learn about the self motion and about the rapid processes creating the remaining collective features. Finally for κ large enough the free atom model (Eqs. 7 and 8) should be approached. In a recent study[39] on *high temperature* liquid lead (1173°K) it seems that such a limit is approached at κ-values of order 7 Å^{-1}. The transform from a diffusive to a free atom behaviour has, however, not been clarified yet.[40]

For $\kappa \sim \kappa_0$ the structural effects dominate in forming $S(\kappa, \omega)$ and its ω-integral $S(\kappa)$. This is well displayed in the intermediate scattering function $F(\kappa, t)$ derived from $S(\kappa, \omega)$ by a Fourier inversion. As for instance clearly shown for liquid rubidium[11] the function $F(\kappa, t)$ decays first very rapidly and then more slowly for κ-values of 1.25 Å^{-1} and 2.00 Å^{-1} on each side of $\kappa = \kappa_0 = 1.50$ Å^{-1}. At this value of κ, $F(\kappa, t)$ decays only slowly showing that the atomic configuration round each atom seen at this wave length has a considerable stability in time (Figure 32). In contrast atoms are more
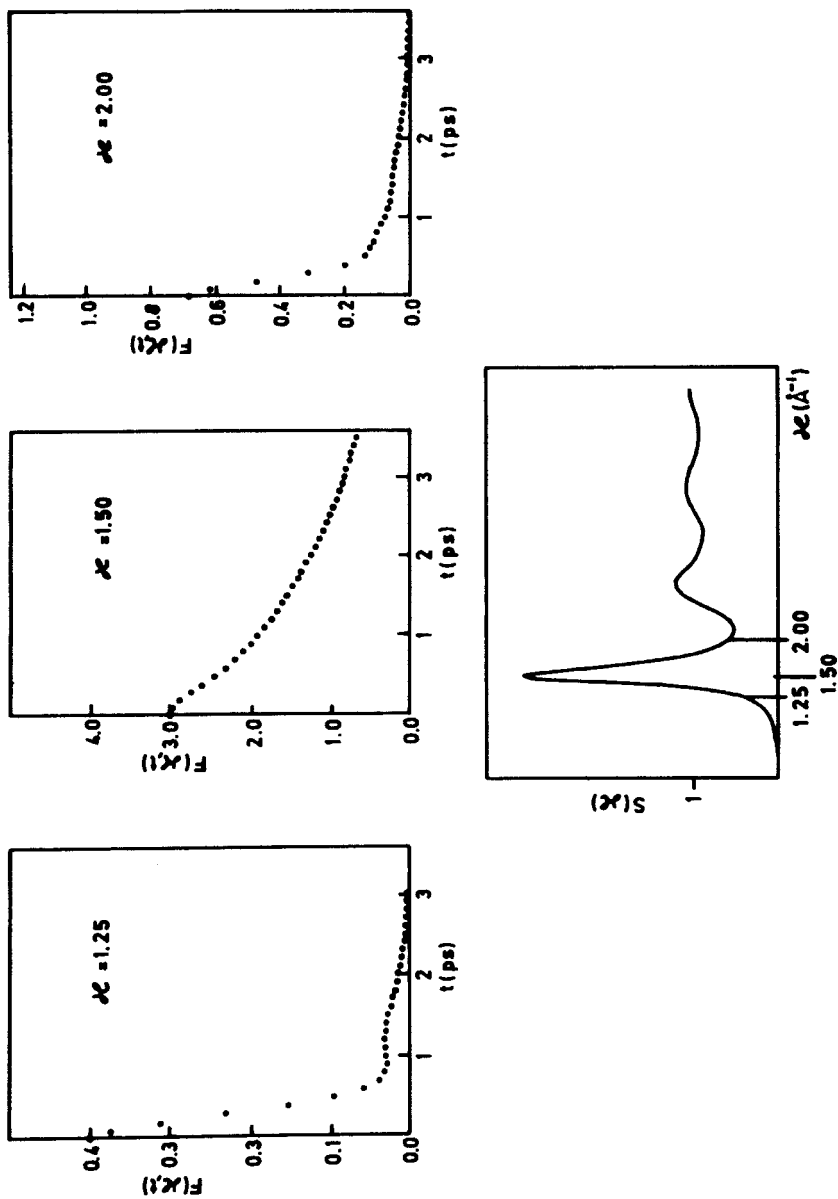
FIGURE 32   Time decay of the intermediate scattering function $F(\kappa, t)$ for liquid rubidium for three selected κ-values 1.25, 1.50 and 2.00 Å^{-1}. For comparison the structure factor of liquid rubidium is also shown. At $\kappa = 1.25$ and 2.00 Å^{-1} $S(\kappa)$ is < 1 and at 1.50 Å^{-1} $S(\kappa)$ has its maximum of about 3 (after J. R. D. Copley and J. M. Rowe, 1974).

quickly thrown out from such configuration which correspond to κ-values of 1.25 and 2.00 Å^{-1}.

It is thus fair to say that for $S(\kappa)$ considerably larger than one, round κ_0, the structural effects dominate in $S(\kappa, \omega)$. For $S(\kappa) \ll 1$ the collective effects tend to dominate in $S(\kappa, \omega)$ and for $S(\kappa) \sim 1$ the self motion of atoms is dominating $S(\kappa, \omega)$.

References

1. L. van Hove, *Phys. Rev.*, **95**, 249 (1954).
2. G. H. Vineyard, *Phys. Rev.*, **110**, 999 (1958).
3. K. E. Larsson, U. Dahlborg and S. Holmryd, *Arkiv f. Fysik*, **17**, 369 (1960). First measurements made November 1957–September 1958 by the Stockholm group.
4. B. N. Brookhouse, T. Arase, G. Caglioti, M. Sakamoto, R. N. Sinclair and A. D. B. Woods, "Crystal Dynamics of Lead," p. 531 in Proc. IEAE Symp. on Inelastic Scattering of Neutrons in Solids and Liquids. Vienna 1960, published 1961.
5. K. E. Larsson, U. Dahlborg and D. Jovic, "Collective Atomic Motions in Liquid Aluminium studied by Cold Neutron Scattering," p. 117 in vol. II of Proc. IAEA Symp. on Inelastic Scattering of Neutrons. Bombay 1964, published 1965. First measurements made October 1958–April 1959 by the Stockholm group. Many other similar studies were made. See for instance S. J. Cocking, *Adv. Phys.*, **16**, 62, 309 (1967); P. A. Egelstaff, *Brit. J. Appl. Phys.*, **16**, 1219 (1965). These references and a review article by K. E. Larsson on p. 397 in Vol. I of Proc. IAEA Symp. on Neutron Inelastic Scattering held in Copenhagen 1968, published in Vienna 1968, give a feeling of the status of the liquid dynamics as seen by neutron scattering until 1968.
6. K. S. Singwi, *Phys. Rev.*, **136**, A969 (1964); *Physica*, **31**, 1257 (1965).
7. P. A. Egelstaff, Harwell Report (1962), AERE—R4101.
8. K. Sköld and K. E. Larsson, *Phys. Rev.*, **161**, 102 (1967).
9. P. D. Randolph and K. S. Singwi, *Phys. Rev.*, **152**, 99 (1966).
10. B. N. Brockhouse and N. K. Pope, *Phys. Rev. L.*, **2**, 287 (1959).
11. J. R. D. Copley and J. M. Rowe, *Phys. Rev.*, **A9**, 1656 (1974).
12. J. R. D. Copley and S. W. Lovesey, "The dynamic properties of monoatomic liquids," *Rep. Prog. in Phys.*, **38**, 461–563.
13. A. Rahman, *Phys. Rev.*, **136**, A405 (1964).
14. D. Levesque, L. Verlet and J. Kurkijärvi, *Phys. Rev.*, **A7**, 1690 (1973).
15. B. J. Alder, D. M. Gass and T. E. Wainwright, *J. Chem. Phys.*, **53**, 3813 (1970).
16. J. P. Boon and S. Yip, *Molecular Hydrodynamics*, McGraw-Hill (1980).
17. K. Sköld, J. M. Rowe, G. Ostrowski and P. D. Randolph, *Phys. Rev.*, **A6**, 1107 (1972).
18. M. W. Johnson, B. McCoy, N. H. March and D. I. Page, *Phys. Chem. Liq.* (GB), **6**, 243 (1977).
19. J. Frenkel, *Kinetic Theory of Liquids*, Dover (1955).
20. L. P. Kadanoff and P. C. Martin, *Ann. Phys.* (*NY*), **24**, 419 (1963).
21. R. Zwanzig and M. Bixon, *Phys. Rev.*, **A2**, 2005 (1970).
22. P. A. Fleury and J. P. Boon, *Phys. Rev.*, **186**, 244 (1969).
23. N. K. Ailawadi, A. Rahman and R. Zwanzig, *Phys. Rev.*, **A4**, 1616 (1971).
24. V. F. Sears, *Can. J. Phys.*, **48**, 616 (1970).
25. J. L. Yarnell, M. J. Katz, R. G. Wenzel and S. H. Koenig, *Phys. Rev.*, **7**, 2130 (1973).
26. H. Bell, H. Moeller-Wenghoffer, A. Kollmar, R. Stockmeyer, T. Springer and H. Stiller, *Phys. Rev.*, **A11**, 316 (1975).
27. O. Söderström, *Phys. Rev.*, **A23**, 785 (1981); O. Söderström, J. R. D. Copley, J. B. Suck and B. Dorner, *J. Phys. F: Metal Phys.*, **10**, L151 (1980).
28. S. W. Haan, R. D. Mountain, C. S. Hsu and A. Rahman, *Phys. Rev.*, **A22**, 767 (1980).

29. Kinetic theory in the present modern meaning was developed mainly by the groups: (a) Mazenko and co-workers (American group), (b) Götze, Lücke and Bosse (West German group), (c) Sjölander and Sjögren (Swedish group). The present presentation follows results obtained by Sjölander and Sjögren: L. Sjögren and A. Sjölander, *J. Phys. C: Solid State Phys.*, **12**, 4369 (1979). L. Sjögren, *J. Phys. C.*, **13**, 705 (1980), L. Sjögren, *Phys. Rev.*, **A22**, 2866, 2883 (1980).

30. L. Sjögren and A. Sjölander, *Ann. Phys.*, **110**, 122, 421 (1978); L. Sjögren, *Ann. Phys.*, **111**, 156, 173 (1978).

31. K. E. Larsson, *Phys. Chem. Liq.*, **9**, 117 (1980).

32. I. Ebbsjö, T. Kinell and I. Waller, *J. Phys. C: Solid St. Phys.*, **13**, 1865 (1980).

33. L. Sjögren, *J. Phys. C: Solid St. Phys.*, **11**, 1493 (1978).

34. W. C. Kerr, *Phys. Rev.*, **174**, 316 (1968).

35. S. Jjödin and A. Sjölander, *Phys. Rev.*, **A18**, 1723 (1978); S. Sjödin, *J. Phys. C: Solid St. Phys.* (1979).

36. B. R. A. Nijboer and A. Rahman, *Physica*, **32**, 415 (1966).

37. G. Wahnström and L. Sjögren, *J. Phys. C: Solid St. Phys.*, **15**, 401 (1982).

38. U. Dahlborg and G. Olsson, *Phys. Rev.*, **A25**, 2712 (1982).

39. O. Söderström, U. Dahlborg and M. Davidovic, *Phys. Rev. A*, **27**, 470 (1983).

40. K.-E. Larsson, *Phys. Chem. Liq.*, **12**, 211 (1983).